

ENGINEERING RESEARCH INSTITUTE
UNIVERSITY OF MICHIGAN
ANN ARBOR

Final Report

THE TWO-FREQUENCY FLAW DETECTOR

L. F. Kazda

John Mau

Project 1685-1

BARNES-GIBSON-RAYMOND DIVISION
ASSOCIATED SPRING CORPORATION
PLYMOUTH, MICHIGAN

June 1955

TABLE OF CONTENTS

	Page
LIST OF TABLES	iv
LIST OF FIGURES	v
OBJECT	vii
ABSTRACT	vii
I. INTRODUCTION	1
II. THE SINGLE-FREQUENCY SYSTEM	2
2.1. The Theory of the Single-Frequency Flaw Detector	2
2.2. Tests Made on the Single-Frequency System by Trained Personnel	3
2.3. Tests Made on the Single-Frequency System by Untrained Personnel	6
III. THE TWO-FREQUENCY SYSTEM	7
3.1. The Need for the Two-Frequency System	7
3.2. The Two-Frequency System	8
3.3. Theory Underlying the Two-Frequency System	8
3.4. The Physical Conception of the Two-Frequency System	14
3.5. Summary of Proposed Theory	14
IV. STUDY OF THE RELATION BETWEEN ELECTRICAL AND PHYSICAL PROPERTIES OF SPRING WIRE	16
4.1. Variation of Resistance and Reactance with Wire Size for Different Chemical Composition	16
4.2. Variation of Resistance and Reactance with Frequency	18
4.3. Variation of Resistance and Reactance with Frequency for a Cracked Sample	18
4.4. Variation of Resistance and Reactance with Two Heats	18
V. THE OPERATION OF THE TWO-FREQUENCY FLAW DETECTOR	22
5.1. Front Panel Layout	22
5.2. Operation of the Flaw Detector	22

TABLE OF CONTENTS (continued)

	Page
5.3. Contour Plots of Chrome-Silicon Wire	25
5.4. Testing Wire Using the Two-Frequency System	28
CONCLUSIONS	31
SUGGESTIONS FOR FUTURE WORK	32
APPENDIX	33
A-1. The General Radio 916 AL Bridge	33
A-2. The High-Frequency Oscillator	33
A-3. High-Frequency Modulator and 1000-Cps Oscillator	36
A-4. The 1.2-Megacycle Pre-amplifier	36
A-5. The Low-Frequency Oscillator	36
A-6. The Low-Frequency Modulator and 400-Cps Oscillator	40
A-7. 500-Kilocycle Pre-amplifiers	40
A-8. The Common Amplifier	40
A-9. The Audio Filter and Difference Amplifier	44
A-10. The Control Chassis	44
A-11. The Meter Circuit	44
A-12. Power Supplies	44
BIBLIOGRAPHY	49

LIST OF TABLES

	Page
2.1 TEST RESULTS OBTAINED BY TRAINED PERSONNEL	5
2.2 TEST RESULTS OBTAINED BY UNTRAINED PERSONNEL	6
5.1 RESULTS OF TESTS WITH THE TWO-FREQUENCY FLAW DETECTOR	30

LIST OF FIGURES (continued)

	Page
A-10. Control Chassis	46
A-11. Meter Circuit	47
A-12. Power Supply Lambda Model 28	48

OBJECT

The purpose of this project is to develop a nondestructive flaw detector that will test wire continuously before any fabrication process has taken place. The detector should be able to detect seams in spring wire stock that are 0.0005 inch deep or deeper. The completed system should be capable of being set to reject seams in commercial wire that are 3 percent of the wire diameter in depth or larger.

ABSTRACT

This report is a summary of the work that has been carried on during the past five years, first on a single-frequency flaw detector and more recently on the two-frequency flaw detector. Included is a brief discussion of the single-frequency system and the results that were obtained using such a system. In addition, the reader will find a theoretical description of the two-frequency flaw detector and some of the results that have been obtained to date using this system. In the conclusions, the advantages and disadvantages of the two-frequency flaw detector will be discussed along with suggestions for future work.

I. INTRODUCTION

At the present time there are three standard methods of detecting flaws in spring wire. They are:

1. sectioning and polishing,
2. etching, and
3. magnafluxing.

In the first method, wire is sectioned and polished using standard metallurgical techniques. It is then inspected under a microscope. Seams of the order of 0.0005 inch can be detected when this process is performed by experienced personnel. In addition, by this method, it is possible to obtain the following qualitative information about a section of the wire:

1. the depth of the seam,
2. the physical nature of the seam, and
3. whether impurities are present in the wire.

The major limitation on this method is that the section being inspected represents the state of the wire at precisely a single point. In order to obtain a true contour of the physical state of the wire it would be necessary to repeat this process many times.

Etching requires a short piece of wire to be immersed in acid for a period of time. After the wire is removed from the acid, the surface is visually inspected under a magnifying glass or microscope; this is a very positive test for deep seams. However, shallow cracks and lap seams can become hard to distinguish from surface scratches.

In the magnaflux process, a direct current is passed axially through a section of wire. The current must be of such magnitude so as to produce a high-current density within the test sample. The current flowing through the test sample causes a large magnetic field to be set up radially within the sample. If the direct current is now removed, the test sample will possess some residual magnetism, a characteristic of all magnetic materials. The magnitude of the residual flux will in general depend on the phys-

ical and chemical properties of the test sample. However, as long as the test sample does not contain a seam, the residual flux will be confined to the wire except at the ends of the sample. If now an axial flaw exists, there will be a leakage flux at the flaw. In order to detect this leakage flux, the test sample is sprinkled with powdered iron. The powder does not stick to the wire except where there is external flux to hold magnetically the powder to the iron. This method of test is very good except for shallow lap seams where very little leakage flux exists and the iron powder may not collect to a degree that can be detected visually.

The three methods described, all of which are used at the present time, are destructive methods of test. Once the sample has been tested it is destroyed. Therefore, it is necessary to employ these tests only as spot checks on wire in general. The objective of this project is therefore to produce a detector that will test wire continuously and nondestructively.

II. THE SINGLE-FREQUENCY SYSTEM

In this section will be found a brief description of the theory underlying the single-frequency flaw detector. Section 2.2 contains a summary of results that were obtained on the single-frequency system when operated by a trained research assistant from the Engineering Research Institute. In section 2.3 will be found a summary of the results that were obtained on the single-frequency system when operated by a production worker from the Cook Plant of the Associated Spring Corporation.

2.1. THE THEORY OF THE SINGLE-FREQUENCY FLAW DETECTOR

One method of detecting axial seams in a wire is dependent on the interruption offered by the seams to a circumferential current flow. Circumferential eddy currents are induced in the wire by inserting it coaxially into a solenoid specifically designed to meet certain requirements. The reactions that these currents offer in the solenoid that induces them will then be a measure of the physical condition of the wire. It has been shown^{1,2} that the eddy-current distribution within a wire sample is given by the following equation:

$$\frac{i_r}{i_0} = e^{-\sqrt{\pi f \mu \sigma} (r - r_0)}, \quad (2.1)$$

where i_0 = circumferential current flow at the surface in amp/m²,

i_e = circumferential current flow at any point r within the surface,
 r = radius of circumferential current flow, i_e , and
 r_0 = radius of the wire.

In order for the presence of a seam to present a major change from "normal" conditions to the detecting equipment, the eddy currents must be confined to a depth comparable to the anticipated crack depth. Inspection of Equation 2.1 reveals that current distribution decreases exponentially inward from the surface with a decrement $(r - r_0) \sqrt{\pi f \mu \sigma}$. This implies the use of radio frequencies so that the induced eddy currents will be predominantly near the surface.

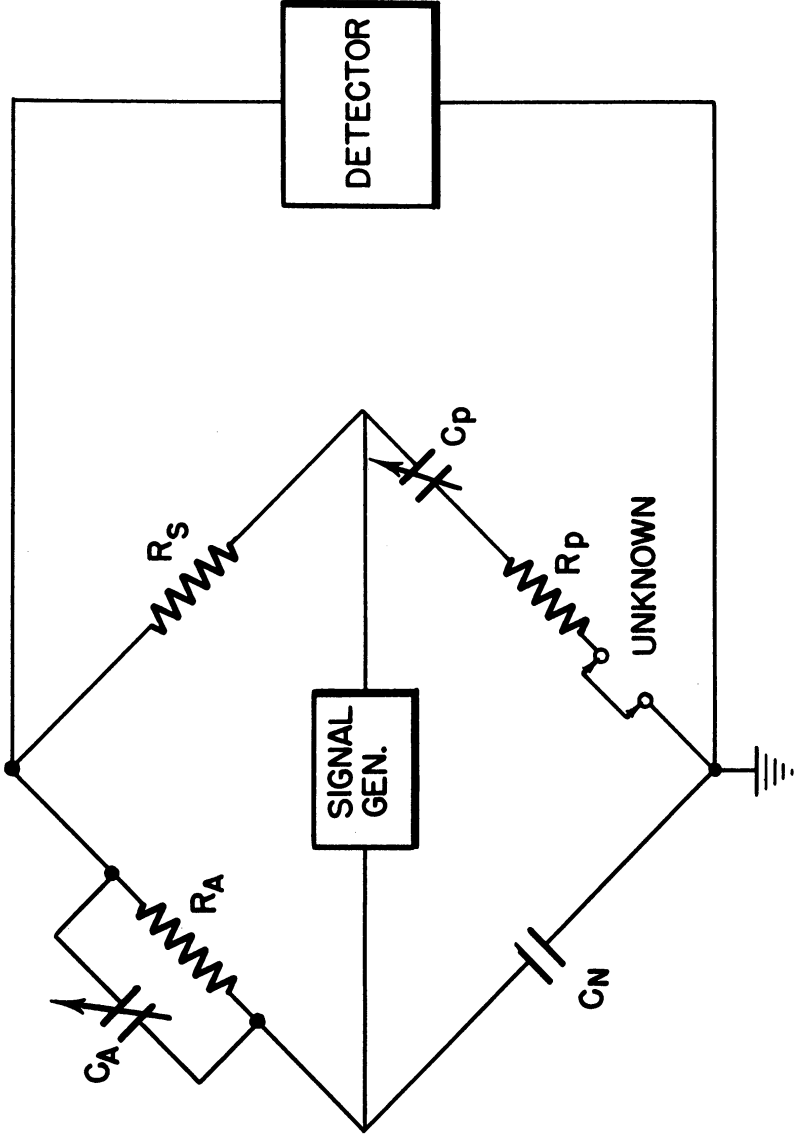
The problem of flaw detection in magnetic materials using radio frequencies is not a new one. A number of investigators have used this approach in one form or another.^{3,4,5} The major differences in the systems have been in the method of measuring the reactions due to the wire.

As a result of the developmental work carried out on the single-frequency system,^{1,2} it was found that General Radio's 916 AL radio-frequency bridge gave the needed voltage sensitivity, long-time stability, and necessary operating range. For excitation, the bridge was supplied by a 500-kc crystal-controlled oscillator. The output from the bridge's detector terminals was amplified, rectified, and indicated on a d-c meter. Operation for automatic marking was provided, using a solenoid-operated paint sprayer. A block diagram of the single-frequency system is shown in Fig. 2.1. A detailed description of the system will be found in progress reports of 1950 and 1951.

2.2. TESTS MADE ON THE SINGLE-FREQUENCY SYSTEM BY TRAINED PERSONNEL

During approximately eight months of operation, 1,000,000 feet of wire were inspected using the single-frequency system. Of this amount, close check was kept on approximately 100,000 feet of various wire sizes. The results of these tests are itemized in Table 2.1. They were obtained by a research assistant of the Engineering Research Institute trained to operate the equipment.

The following remarks may be made regarding the tests shown in Table 2.1. Heat numbers B23332 and B23285 had extremely rough surfaces and appeared to be too hard since many of the bundles were broken into small pieces. The meter deflection varied rapidly and over a wide range of values, indicating many surface deformities such as scale and scratches. With the detector set to indicate seams of the order of 0.003 inch, often the combination of very rough surface and changing ferromagnetic properties caused the detector to indicate seams where none existed. There were sixteen indications



BASIC CIRCUIT DIAGRAM OF TYPE 916 AL R F BRIDGE

Fig. 2.1.

TABLE 2.1

TEST RESULTS OBTAINED BY TRAINED PERSONNEL

Size	Type	Length ft	Heat No.	No. of Indications	No. of Flaws	Depth of Flaws, in.	Deflection Above Avg., unit
<u>Washburn Wire Company Stock</u>							
.1055	Cr Si*	3,367	B23332				
.1055	Cr Si	5,960	B23332	5	1	.003	8
					1	Scratch	8
.1055	Cr Si	3,367	B23332	3			8
.1055	Cr Si	6,532	B23332				
.1055	Cr Si	6,400	B23332	2			8
.1055	Cr Si	7,239	B23332	2			8
				2	2	.009	15
.1055	Cr Si	7,509	B23332				
.1055	Cr Si	6,936	B23332				
.1055	Cr Si	6,936	B23285	3	1	Scratch	8
.1055	Cr Si	7,104	B23285	1			8
.1055	Cr Si	7,171	B23285				
.1055	Cr Si	6,268	B23285				
.135	Cr Si	28,000	B23406				
			B23332	1	1	.007	15
.0625	Cr Si	16,000		2	1	.0006	8
<u>American Steel and Wire Company Stock</u>							
.080	Cr Si	10,000	6112	5	1	.004	8
					1	.009	10
					1	.031	27
					1	.035	32

*Chrome silicon.

in 78,000 feet of 0.1055-inch chrome silicon, with only three flaws, and a deflection of eight units above average. With wire that has a rough surface, the detector cannot be relied on to indicate only flaws when set for such small seams. In addition, 28,000 feet of 0.135-inch wire were run with the marking system set to operate at fifteen units deflection, and the one indi-

cation was a flaw, which suggests that with the detector set that high, only flaws will be detected.

The 0.080-inch wire had a smooth surface, and it was very easy to obtain the "dynamic balance." The variations in the depths of the seams will give some idea of the calibration needed for this size of wire. The cracks of 0.004 and 0.009 inch were of short length and could have been caused from cooling strains set up during the processing of the wire. The cracks of 0.031 and 0.035 inch were very long and were probably seams in the original billet from which the wire was drawn. These tests were performed by a research assistant from the Engineering Research Institute.

2.3. TESTS MADE ON THE SINGLE-FREQUENCY SYSTEM BY UNTRAINED PERSONNEL

The remaining 900,000 feet were tested using the single-frequency system, but operated by a production worker from the Cook Plant of the Associated Spring Corporation. Records were kept on 328,000 feet of the various types of wire tested. They are summarized in Table 2.2. Inspection of these results indicates that the machine was detecting surface scratches in addition to the flaws. In addition, a seam 65 feet long was detected in one heat

TABLE 2.2

TEST RESULTS OBTAINED BY UNTRAINED PERSONNEL

Size	Type	Length, ft	Heat No.	No. of Indications	Depth of Flaws
.135	Cr Van*	71,600	21G20	2	
.177	A/C Van**	36,700	22B465	1	
.135	Cr Van/	37,000	23B296	2	
.135	Cr Si	53,600	A11876	2	
				One piece 65 ft long	A seam but not sectioned
.135	Cr Si	17,800	BA23750	0	
.135	Cr Si	9,140	B23748	36	All die scratches
.125	Cr Si	104,200	38816	70	All die scratches

*Chrome vanadium.

**A/C vanadium.

/ Chrome vanadium.

of 0.135-inch-diameter chrome silicon. Individual data on the remaining heats were not available. Since 100% magnaflux was performed on all the chrome-vanadium wire tested by the flaw detector, the magnaflux test served as an excellent check on the reliability of the machine. Out of approximately 100,000 fabricated items made from this wire, the detector failed to detect 4 springs that contained seams. However, the machine rejected 5 drums of what would be considered commercially acceptable spring wire, i.e., wire containing die scratches and nonhomogeneous material structure. Since the marking system was capable of malfunctioning, and since the system was dependent on a human operator, this degree of failure is considered within the limit of expected error.

In summarizing the tests on the single-frequency system, the following statements can be made:

1. The single-frequency system will detect flaws in steel wire.
2. The machine can be operated by a production worker with little training.
3. It is much easier to magnaflux 5 drums of questionable springs rather than 100,000 of them, or, the money saved in eliminating the magnaflux operation would pay for the 5 drums of questionable springs that could be junked as wire prior to fabrication.

III. THE TWO-FREQUENCY SYSTEM

The purpose of this section is to acquaint the reader with the theory underlying the two-frequency system of flaw detection. A brief description of the circuit configuration necessary to perform simultaneous tests on a given sample is given; detailed descriptions of each circuit will be found in the Appendix.

3.1. THE NEED FOR THE TWO-FREQUENCY SYSTEM

In order to balance the bridge in the single-frequency system, it was necessary to balance the bridge on a "good piece" of wire. In trying to find a "good piece" of wire from tests conducted on various wire samples, it was found that the bridge balance was not only sensitive to axial seams within the wire, but also to the following wire properties:

1. wire diameter
2. wire temperature, and
3. wire physical properties:
 - a. hardness,
 - b. microstructure, and
 - c. composition.

Thus, in choosing a single section of wire on which to balance the detector, changes in any of the above properties would also cause the bridge to become unbalanced. If the bridge is balanced on any single section of wire, it would become more and more unbalanced as the wire being tested passes continually through the test solenoid due to the changes in its homogeneous properties. As the bridge becomes unbalanced, it loses its detecting ability. In order for the system to be able to detect small flaws, it was necessary to keep the bridge near balance. This was accomplished by establishing a "running balance," that is, the system was balanced on an average value of the first 100 feet of each bundle. In this way variations through a bundle were kept at a minimum. Thus for every wire bundle a new "running balance" was established on the bridge in order to eliminate the variations in bridge balance that were caused by changes in heat treatment and chemical composition. The variations within a single bundle were much less than the variations obtained in moving from bundle to bundle. It was recognized at this point that a single setting, indicating either wire size and/or chemical composition, would not be possible using the single-frequency system. In order to circumvent the problem of system sensitivity, depending on the physical nature of the wire, the two-frequency system was conceived.

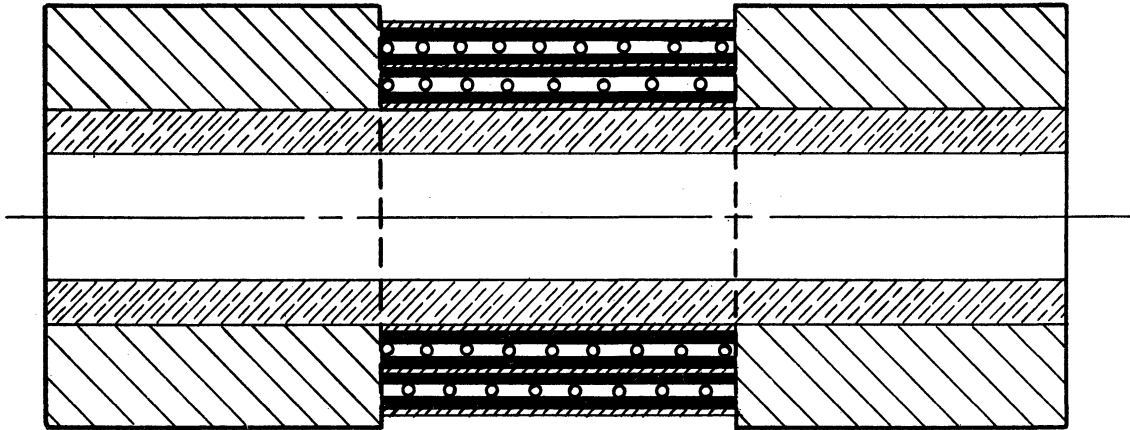
3.2. THE TWO-FREQUENCY SYSTEM

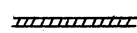
In the single-frequency system the wire to be tested is passed through a solenoid that is located inside the gage head shown in Fig. 2.1. The solenoid is the sensing element of the system. The reactions produced by changes in wire properties are transmitted to the radio-frequency bridge as impedance change in the solenoid. In Fig. 3.1 is shown a solenoid that has been modified by the addition of a second concentric coil. It is possible to measure the reactions produced in this second coil by a second bridge excited by a second frequency similar to the one used in the single-frequency system.

Having a second system working in parallel with the first and testing the same section of wire makes it possible to compare the reactions obtained by either a physical or a chemical change within the test sample. If the outputs of the two systems can be adjusted so that when they are compared they will be zero for homogeneous changes and nonzero for other variations, a perfect detecting system will be obtained. The theory predicting the operation of the two-frequency system using the concentric solenoid shown in Fig. 3.1 is discussed in the following section.

3.3. THEORY UNDERLYING THE TWO-FREQUENCY SYSTEM

It was shown that the actual solenoid containing a wire can be approximated by the equivalent circuit of Fig. 3.2.



 COPPER SHIELD - .005" SHEET
 (NOTE: OPEN CIRCUIT TO EDDY CURRENT FLOW)

 POLYSTYRENE INSULATION - .010" SHEET

 #37 ENAMELED WIRE

 No. 00 PORCELAIN OR QUARTZ TUBING

SCALE: ENLARGED 2 TIMES
 GAGE HEAD

Fig. 3.1.

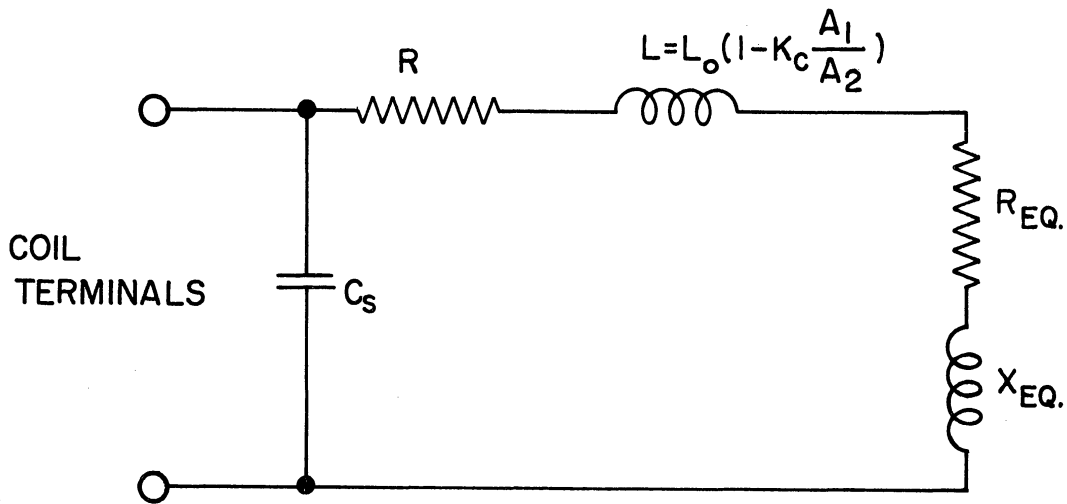


Fig. 3.2. The Single-Frequency Equivalent Circuit of the Gage Head Solenoid.

- where C_s = shunt capacitance,
- R = self-resistance of coil,
- L = self-inductance of coil,
- R_{eq} = the equivalent resistance reflected into the coil by the wire being tested, and
- X_{eq} = the equivalent reactance reflected into the coil by the wire being tested.

Now R_{eq} and X_{eq} were found to be, respectively,

$$R_{eq} = 2\pi r^2 r_o l \sqrt{\frac{\pi f \mu}{\sigma}} \quad \text{and} \quad (3.1)$$

$$L_{eq} = \frac{2\pi n^2 r_o l}{\omega} \sqrt{\frac{\pi f \mu}{\sigma}} ; \quad (3.2)$$

or

$$X_{eq} = 2\pi n^2 r_o l \sqrt{\frac{\pi f \mu}{\sigma}} \quad (3.3)$$

- where r_o = wire radius,
- ω = angular frequency,
- f = cyclical frequency,
- μ = permeability,
- σ = conductivity, and
- l = length of coil.

Inspection of Equations 3.1 and 3.3 reveal that both the resistance and reactance components introduced by the core are proportional to the diameter $\times \sqrt{f\mu/\sigma}$. Therefore, for a given sample at a given frequency, the change in impedance that will unbalance the bridge from a given balance position due

to a change in $\sqrt{\mu/\sigma}$ is

$$\Delta Z_p = k d (\Delta \sqrt{\frac{\mu}{\sigma}}). \quad (3.4)$$

If, on the other hand, the test-sample wire diameter is considered a variable,

$$\Delta Z_d = k \sqrt{\frac{\mu}{\sigma}} \Delta d. \quad (3.5)$$

The ratio formed by Equations 3.4 and 3.5 yield:

$$\frac{\Delta Z_p}{\Delta Z_d} = \frac{d \Delta \sqrt{\frac{\mu}{\sigma}}}{d \Delta \sqrt{\frac{\mu}{\sigma}}} = \frac{\Delta \sqrt{\frac{\mu}{\sigma}}}{\frac{d \Delta}{d}} \quad (3.6)$$

Inspection of Equation 3.6 reveals that for the same percentage change $\sqrt{\mu/\sigma}$ as in the diameter, the impedance changes are equal. Tests made on different samples at that time showed that material property effects give an output voltage variation of about three times the variation due to a change in diameter from 0.131 to 0.125 inch. The $\sqrt{\mu/\sigma}$ was found to vary ordinarily

$$3 \times \frac{0.006}{0.131} = 1.4\%$$

based on the assumption that the change in bridge unbalance was small, and therefore an approximately linear relation exists between the change in impedance and output voltage.

Consideration of the above relationship led to the idea of the two-frequency system. If measurements could be taken simultaneously on a wire sample in such a manner that they would be affected similarly by the material properties but dissimilarly by seams, the effects of materials could be eliminated. In order to measure the same wire sample at two different frequencies simultaneously, concentric solenoids were used, connected in a manner shown in Fig. 3.1.

Under these conditions the equivalent impedance that the high-frequency bridge "sees" will be

$$Z_{eqh} = k_h d_1 \sqrt{f_h} \sqrt{\frac{\mu}{\sigma}}, \quad (3.7)$$

while the low-frequency bridge will "see"

$$Z_{eq1} = k_1 d_1 \sqrt{f_1} \sqrt{\frac{\mu}{\sigma}}. \quad (3.8)$$

To use the system, two "good" samples are needed which differ in $\sqrt{\mu/\sigma}$, or in effect differ in their material properties. Using one of the samples as a standard, both bridges are balanced so that the output voltage is zero. When the other sample is inserted into the gage head for calibration, both bridges will become unbalanced, yielding output voltages on each channel. The amplifiers of the two channels are then adjusted so that the output voltages are equal. The bridges were balanced on the initial sample. Let their impedances be represented by

$$Z_{h1} = k_h d_1 \sqrt{f_h} \sqrt{\frac{\mu_1}{\sigma_1}} \quad \text{and} \quad (3.9)$$

$$Z_{11} = k_1 d_1 \sqrt{f_1} \sqrt{\frac{\mu_1}{\sigma_1}}. \quad (3.10)$$

The second sample introduces a change in equivalent impedance represented by

$$Z_{h2} = k_h d_2 \sqrt{f_h} \sqrt{\frac{\mu_2}{\sigma_2}} \quad \text{and} \quad (3.11)$$

$$Z_{12} = k_1 d_2 \sqrt{f_1} \sqrt{\frac{\mu_2}{\sigma_2}}. \quad (3.12)$$

If the bridges output voltages change linearly for changes in impedance from the balance conditions and if the amplifiers are linear, the output voltages are represented by

$$E_{h2} = k_h \left[d_2 \sqrt{f_h} \sqrt{\frac{\mu_2}{\sigma_2}} - d_1 \sqrt{f_h} \sqrt{\frac{\mu_1}{\sigma_1}} \right] \quad \text{and} \quad (3.13)$$

$$E_{11} = k_1 \left[d_2 \sqrt{f_1} \sqrt{\frac{\mu_2}{\sigma_2}} - d_1 \sqrt{f_1} \sqrt{\frac{\mu_1}{\sigma_1}} \right]. \quad (3.14)$$

Now adjusting the amplifier gains until $E_{h2} = E_{l1} = 1$ volt, then

$$k_h = \frac{1}{\left[d_2 \sqrt{f_h} \sqrt{\frac{\mu_2}{\sigma_2}} - d_1 \sqrt{f_h} \sqrt{\frac{\mu_1}{\sigma_1}} \right]} \text{ and} \quad (3.15)$$

$$k_l = \frac{1}{\left[d_2 \sqrt{f_l} \sqrt{\frac{\mu_2}{\sigma_2}} - d_1 \sqrt{f_l} \sqrt{\frac{\mu_1}{\sigma_1}} \right]} \quad (3.16)$$

Now, for another good sample, the output voltage would be given by

$$E_{h3} = k_h \left[d_3 \sqrt{f_h} \sqrt{\frac{\mu_3}{\sigma_3}} - d_1 \sqrt{f_h} \sqrt{\frac{\mu_1}{\sigma_1}} \right] \text{ and} \quad (3.17)$$

$$E_{l3} = k_l \left[d_3 \sqrt{f_l} \sqrt{\frac{\mu_3}{\sigma_3}} - d_1 \sqrt{f_l} \sqrt{\frac{\mu_1}{\sigma_1}} \right] \quad (3.18)$$

Substitution of k_h and k_l from Equations 3.17 and 3.18, yield an output ratio

$$\frac{E_{h3}}{E_{l3}} = 1 \quad (3.19)$$

Thus, once the bridges have been balanced and calibrated on two "good" samples, the output voltages will be equal for any other good sample.

A cracked sample, however, cannot be considered homogeneous. A crack decreases the conductivity (σ) since it interposes a barrier into the path of current flow. The eddy currents are effectively in different depths and therefore the conductivity of the two channels is different. Since a greater portion of the current path is interrupted by the shallower current (high frequency) than by the deeper current (low frequency), there will be a greater change in the conductivity of the shallower current. Therefore, for a cracked sample

$$\left[\sqrt{\frac{\mu_4}{\sigma_4}} \right]_h > \left[\sqrt{\frac{\mu_4}{\sigma_4}} \right]_l \quad (3.20)$$

This results in the voltages being unbalanced in the following fashion:

$$\frac{E_{h4}}{E_{l4}} = \frac{\frac{d_4}{d_1} \left(\left[\frac{\mu_4}{\sigma_4} \right]_h - \left[\frac{\mu_1}{\sigma_1} \right] \right)}{\frac{d_4}{d_1} \left(\left[\frac{\mu_4}{\sigma_4} \right]_l - \left[\frac{\mu_1}{\sigma_1} \right] \right)} > 1 . \quad (3.21)$$

Equation 3.21 shows that the voltage out of the high-frequency bridge will be greater than out of the low-frequency bridge. Thus in order to detect cracks it is only necessary to discern when there is a difference in output voltages.

3.4. THE PHYSICAL CONCEPTION OF THE TWO-FREQUENCY SYSTEM

In Fig. 3.3 is shown a block diagram of the two-frequency flaw detector with the carrier frequencies set at .5 and 1.2 mc. Inspection of Fig. 3.3 reveals that the system consists of a high- and a low-frequency radio-frequency oscillator that is modulated by a 1000 and 400 cps audio frequency. The two modulated signals are connected to generator terminals of the high- and low-frequency bridges. Each bridge has as its unknown a coil from the gage-head solenoid. The outputs from the detector terminals of the two bridges are demodulated and passed through a common audio amplifier. After passing through a common amplifier, they are separated, rectified, and then compared at the output of the difference detector. The output from the difference amplifier operates a trigger circuit that controls the operation of a spray gun. Visual indication is obtained by connecting a vacuum-tube voltmeter across the difference-detector terminals.

The use of a common amplifier assured the same relative gains in the high- and low-frequency channels. When modulated signals are used, the carrier frequencies can be changed while the audio amplifying section remains unchanged.

A comparison of this diagram with the block diagram of the single-frequency flaw detector shown in Fig. 2.1 reveals that in reality the two systems are similar when each channel is considered separately, the major difference between them being the use of a modulated radio-frequency signal to supply the system.

3.5. SUMMARY OF PROPOSED THEORY

It was theorized in the two-frequency system that a homogeneous change within the wire under test would result in equal changes in bridge out-

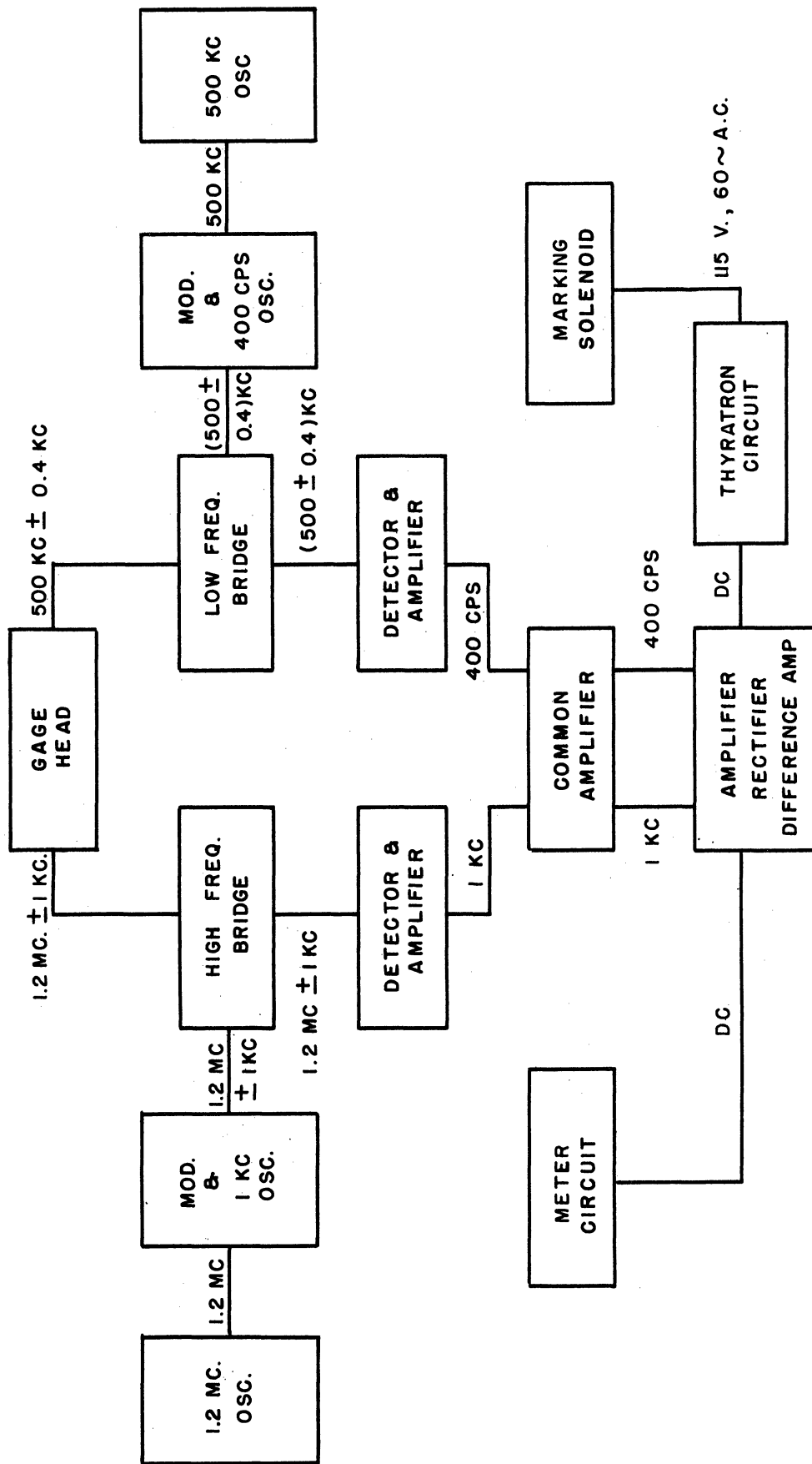


FIG. 3.3 BLOCK DIAGRAM FOR TWO FREQUENCY WIRE FLAW DETECTOR

put voltage. The net change in voltage between the two systems would be the same. If a circuit were constructed so as to measure the difference voltage, this meter would read zero. On the other hand, if a flaw were present within the wire under test, the high-frequency bridge would become unbalanced by a larger amount than the low-frequency bridge. This would result in a difference voltage which would be indicated on the meter. In order to verify the above theory, numerous tests have been conducted during the past 9 months on the prototype two-frequency system shown in block form in Fig. 3.3. The results of the tests made on the system are summarized in part V.

IV. STUDY OF THE RELATION BETWEEN ELECTRICAL AND PHYSICAL PROPERTIES OF SPRING WIRE

In order to determine what relations exist between the physical and chemical properties of spring wire and their corresponding electrical properties, a number of tests were performed on samples of wire of various sizes and composition. While it would have been desirable to conduct some of these tests earlier in the development of the system, only recently were a large number of random heats, sizes, and composition available. The following results were found to exist between the material properties of the wire and their electrical properties. The results of these tests are presented in this section.

4.1. VARIATION OF RESISTANCE AND REACTANCE WITH WIRE SIZE FOR DIFFERENT CHEMICAL COMPOSITION

Inspection of the curves in Fig. 4.1 reveals that the electrical reactance of the high- and low-frequency systems varies approximately 2 to 3% as the wire diameter is changed from 0.080 to 0.208 inch. Inspection of the curves shows that a difference of approximately 1% exists between the three types of wire tested, namely, T-chrome silicon, T-chrome vanadium, and T-valve. On the contrary, one finds that the resistance as "seen" by the bridge changes 57% with the same change in wire diameter. The slope of the resistance curves, $\Delta R/\Delta d$, for the three compositions were almost the same. These curves are average values of a number of tests.

Inspection of the curves for T-valve shows a very irregular curve. If points on this curve are connected for samples having constant silicon content, a smooth curve results that is almost parallel to the resistance curves of T-chrome silicon or T-chrome vanadium (see dashed line). When properly adjusted, the flaw detector could be used for detecting small changes in the silicon content of spring stock.

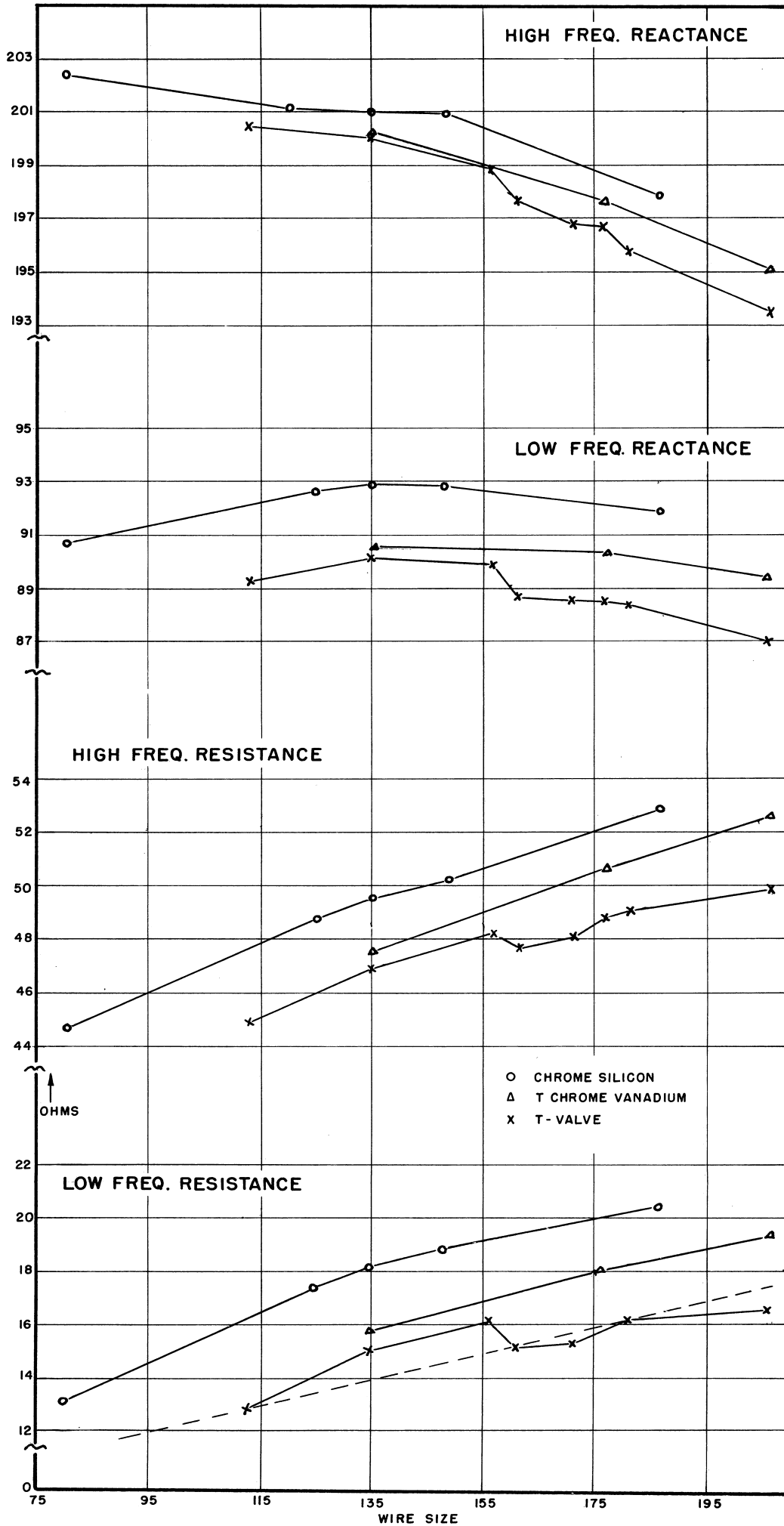


Fig. 4.1. Electrical Characteristics of Various Spring Wires

4.2. VARIATION OF RESISTANCE AND REACTANCE WITH FREQUENCY

In Fig 4.2 will be found a comparison of the resistance and reactance found to exist for samples of T-chrome silicon, T-chrome vanadium, and T-valve, all having a diameter of 0.135 inch. Inspection of these curves reveals that as a function of frequency their reactances are practically identical (variation of approximately 2% at each frequency). Inspection of the resistance curves reveals that considerable difference exists in the resistance of samples having the same wire diameters but different chemical composition.

4.3. VARIATION OF RESISTANCE AND REACTANCE WITH FREQUENCY FOR A CRACKED SAMPLE

In Fig. 4.3 will be found a comparison of the resistances and reactances that are seen by the bridge for a good section of 0.080-inch-diameter wire and a section of 0.080-inch-diameter wire that has a 0.020-inch crack. Inspection of the reactance curves reveals that a 0.020-inch seam in a wire does not change its reactance. However, it will be noted that the resistance of the wire in this case has increased from 2 to 8%. It can also be seen that the difference between the two resistance curves increases with frequency. This increase of the difference resistance between the two resistance curves is due to the shallower depth of eddy currents at the higher frequencies.

4.4. VARIATION OF RESISTANCE AND REACTANCE WITH TWO HEATS

The plot of Fig. 4.4 was made using two samples of 0.182-inch-diameter T-valve wire. The resistance curves show the difference that exists in their electrical characteristics in going from one heat to another. Comparison of Figs. 4.4 and 4.3 reveals that the difference that exists in the electrical characteristics between two heats is of the same order of magnitude as the difference between a cracked and a good sample of wire. The crack in the sample of Fig. 4.3 is a large visual crack of about 0.020 inch in depth. It is apparent that in passing from one heat to another in a continuous test all but the very largest cracks will be masked unless the system is rebalanced on each new heat.

In the case of the two heats used in Fig. 4.4, the silicon content as analyzed was found to be the same, i.e., 0.22%. It is known that the variation of silicon content is a major factor in producing a detectable difference between heats. From tests conducted to date, it is apparent that other composition properties of the wire, in addition to silicon, affect its elec-

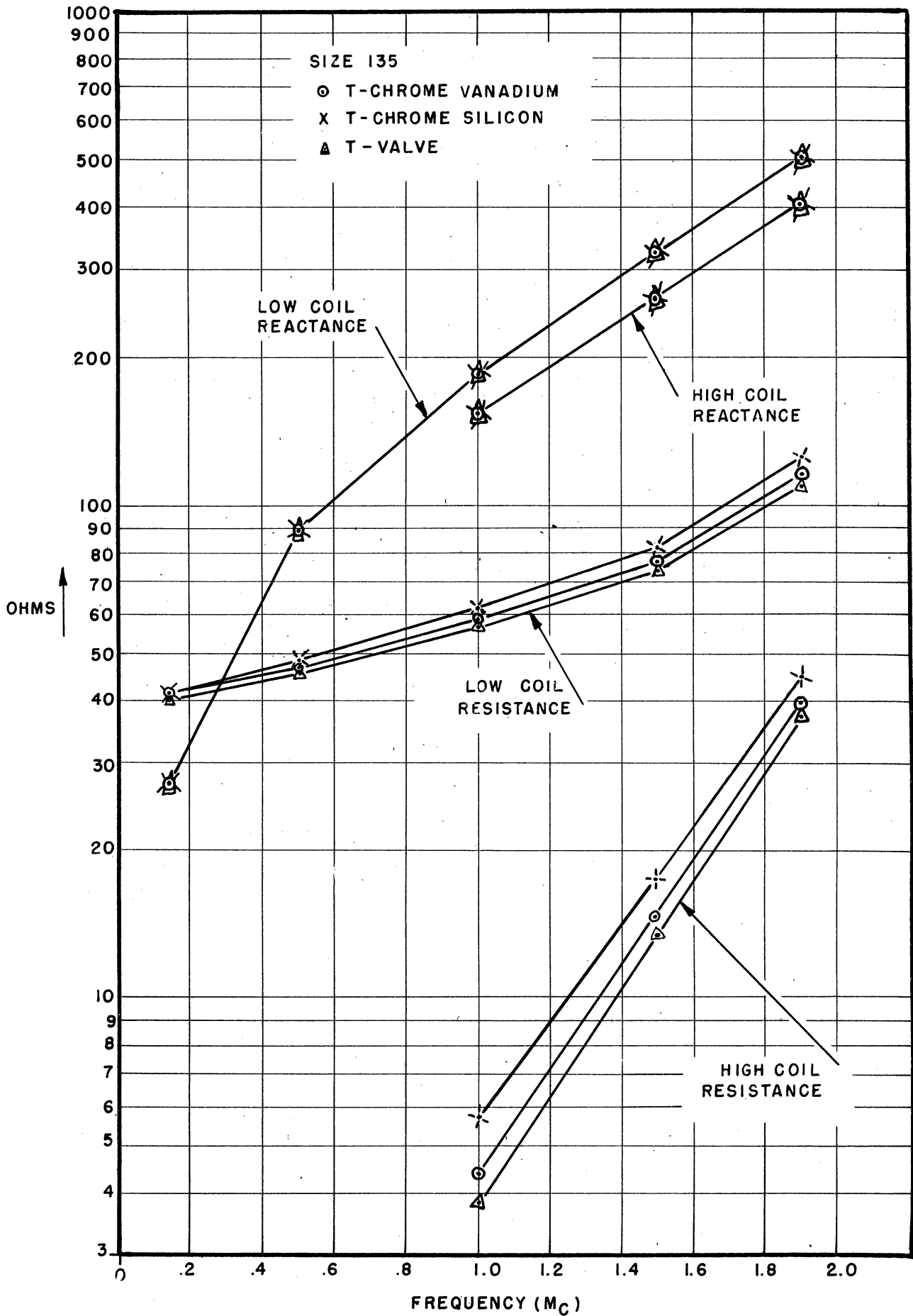


FIG. 4.2 VARIATION OF RESISTANCE AND REACTANCE WITH COMPOSITION

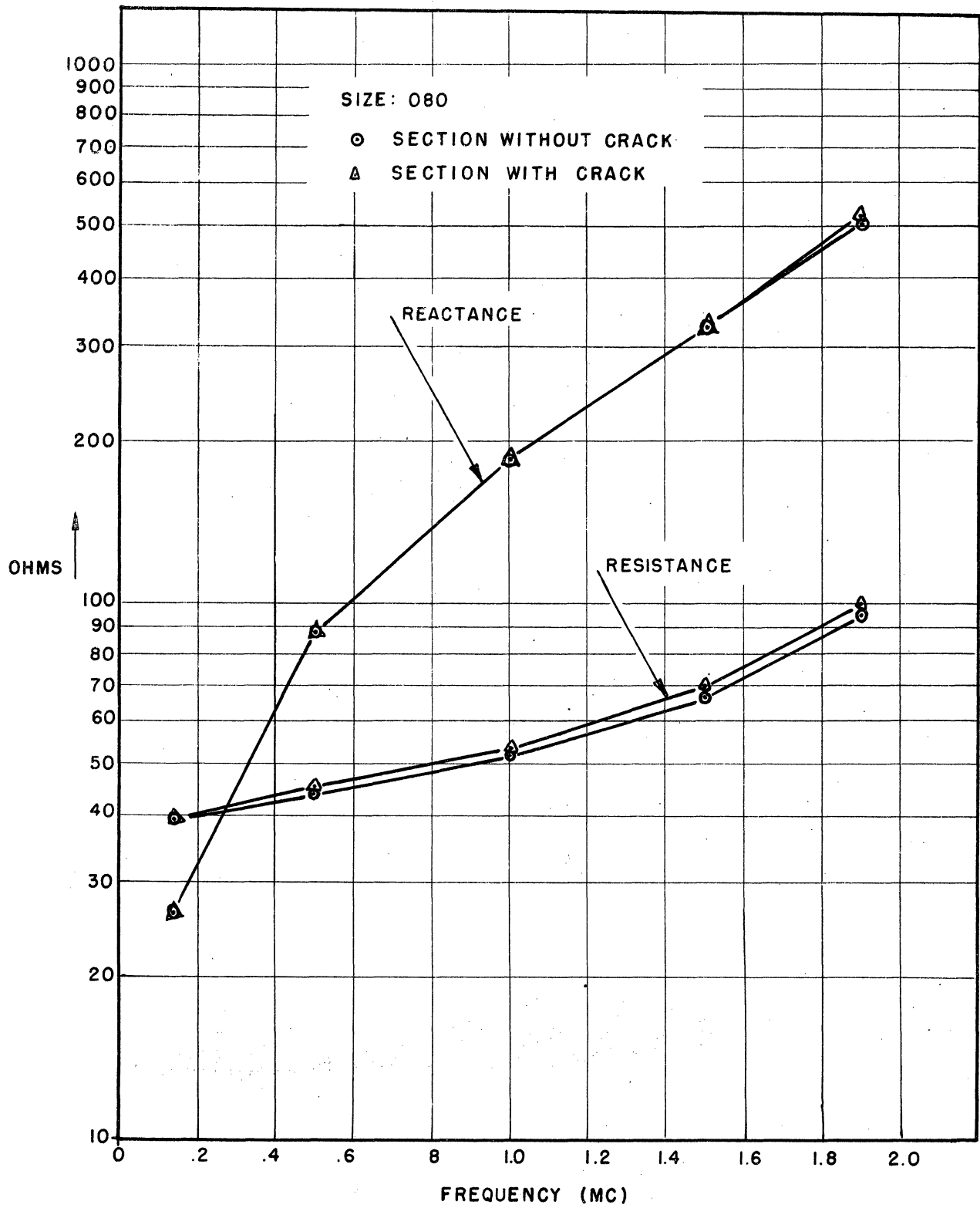


FIG. 4.3 VARIATION OF REACTANCE AND RESISTANCE WITH A CRACKED SAMPLE

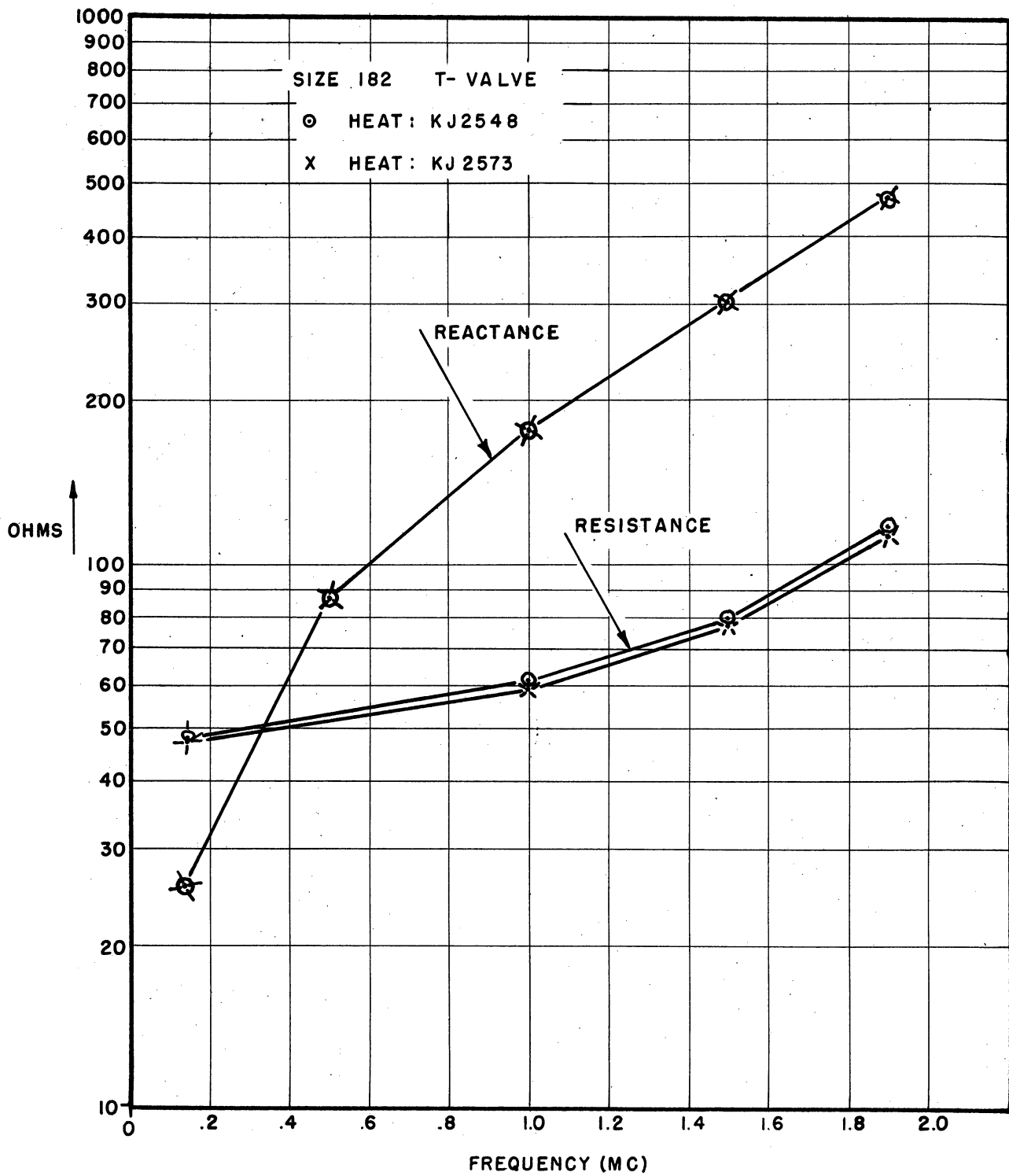


Fig. 4.4. Variation of Resistance and Reactance for Two Heats.

trical properties. However, no exhaustive tests were made to determine the qualitative correlation that exists between the changes in electrical resistance and reactance and changes in chemical composition.

It is conceivable that a system similar to the two-frequency system could be used to detect changes in chemical composition to a finer degree than would be possible by chemical analysis.

V. THE OPERATION OF THE TWO-FREQUENCY FLAW DETECTOR

In this section will be found a brief description of the operation of the two-frequency flaw detector as a guide for those who may wish to use it in the future. In addition will be found a description of contour plots that have been made on the system. This section is concluded by a description of the tests that have been made using the systems and a summary of the results.

5.1. FRONT PANEL LAYOUT

In Fig. 5.0 will be found a diagram of the front panel of the two-frequency system showing the position of all controls. All major controls have been brought out on the front panel for accessibility. Inspection of Fig. 5.0 reveals that all high-frequency components are located on the left while all low-frequency components are located on the right. The power supplies for the system are located on the bottom shelves of the unit. Above the power supplies will be found the high- and low-frequency modulators and oscillators. Above the oscillators are the two radio-frequency bridges. The top panels on each side contain the controls that operate the system once it is calibrated. On page 24 will be found an index to all the controls listed on the front panel.

5.2. OPERATION OF THE FLAW DETECTOR

In order to make measurements on the two-frequency system the following procedure should be followed:

1. Energize the system and allow a "warm-up" period of about an hour in order for the system to reach thermal equilibrium.
2. To calibrate either bridge, a shorting stub of 213 ohms is inserted into the "unknown" terminals of the bridge. The main

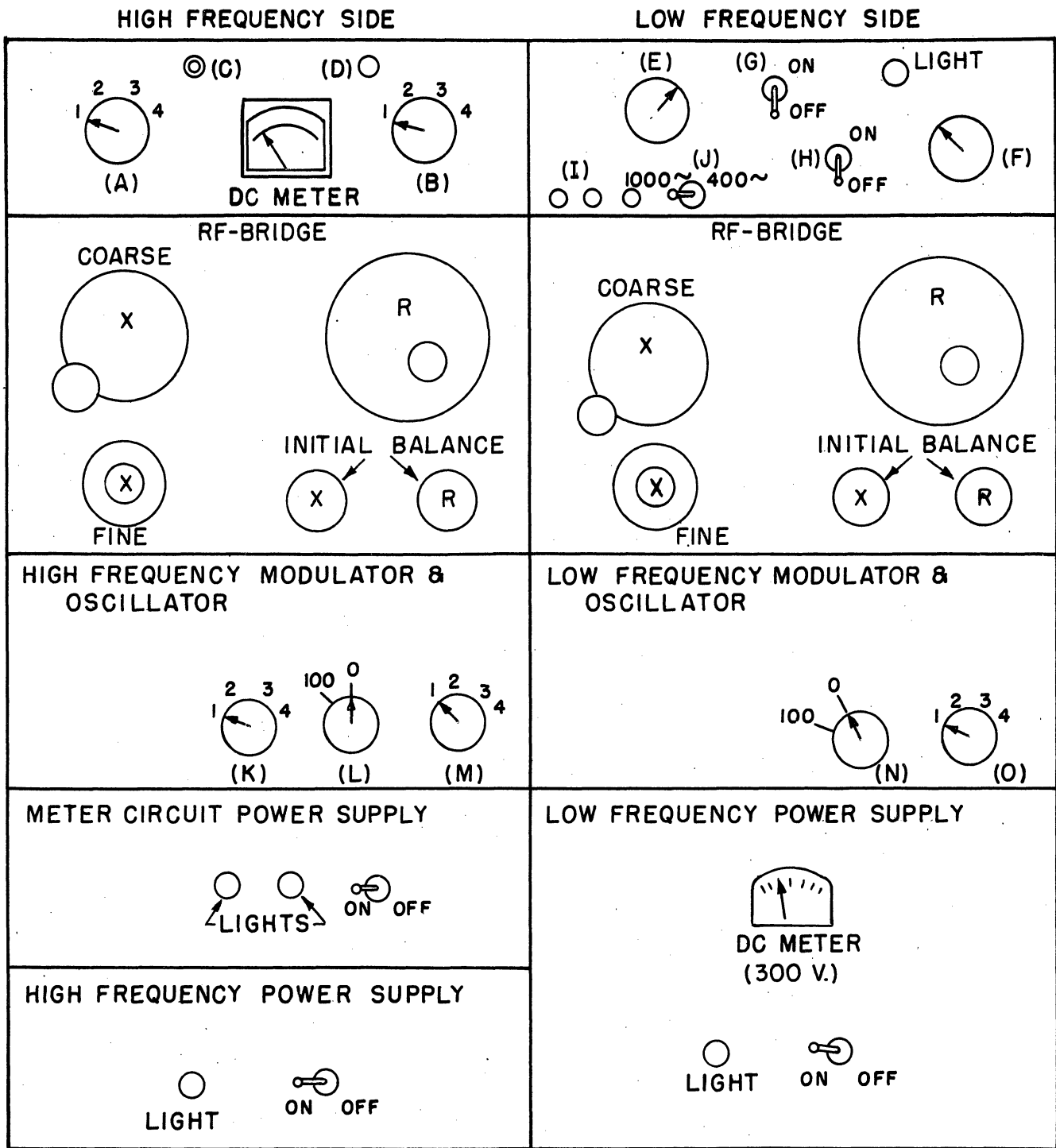


FIG. 5.0 FRONT PANEL LAYOUT

Index to Front Panel Layout (Fig. 5.0)

- (A) D-C Meter Selector Switch
 - Position 1: Low-Frequency Voltage
 - Position 2: High-Frequency Voltage
 - Position 3: Difference Voltage
- (B) Meter Sensitivity Switch
- (C) Meter Button (Push to Read)
- (D) Meter Zero Adjust Screw
- (E) Trigger Voltage Control (Fine Adjustment)
- (F) Trigger Voltage Control (Coarse Adjustment)
- (G) Thyatron Circuit On-Off Switch
- (H) Solenoid On-Off Switch
- (I) Terminal Posts for 1000 and 400 Cps to A-C Meter
- (J) A-C Meter Selector Switch (1000 or 400 Cps)
- (K) Modulator-Frequency Selector Switch
- (L) Gain Control
- (M) Oscillator-Frequency Selector Switch
- (N) Gain Control
- (O) Oscillator-Frequency Selector Switch

R and X dials are then set to zero and the bridge is balanced by means of the initial balance dials. In order to prevent a false balance due to overloading of the amplifiers, the gain should be set low at first and increased as balance is reached. Both bridges are initially balanced in this manner.

3. With both bridges calibrated, the test sample is inserted into the gage head and the bridges are again balanced using only the main R and X dials. The "initial balance" dials are never moved except when the bridges are being calibrated (as in 2 above).
4. The main dials now read the effective resistance and reactance of the solenoid plus the wire test sample.

In order to obtain the contour plots shown in Fig. 5.1, the wire sample being tested (normally a long piece of wire) is moved from section to section and the bridges are balanced on each section thus obtaining an impedance reading for each section. Care is required in balancing the bridges since they are rather critical to operate due to the high system gain. In order to perform the balancing operations, a "feel" must be developed. Once the bridges have been calibrated, however, little difficulty should be encountered as the wire is moved from section to section.

For continuous testing, the bridges do not require calibration, but it is required that they be balanced on a good piece of wire. Full gain is used on the low-frequency channel but the gain switch of the high-frequency side should be set from about 78 to 80. With a good piece of wire in the test coil, the bridges balanced, and the amplifier gain properly set, the voltages of the difference amplifier are adjusted to zero volts. This is done by an adjustment knob on the back of the panel. The system is now ready for operation using the indicating meter as visual indication.

In order to set the trigger circuit to operate the spray gun at the proper instant, the trigger circuit must be calibrated. In order to calibrate it, a wire that is known to have approximately a 0.004-inch crack is inserted in the test coil. This will produce a difference voltage at the input terminal of the thyatron circuit. The "trigger-voltage-control" knobs are then adjusted to just trigger with the difference voltage that is caused by this 0.004-inch crack. The wire that is used for calibration must be of the same heat and composition. In addition, it would be desirable if it were from the same coil.

5.3. CONTOUR PLOTS OF CHROME-SILICON WIRE

One equivalent picture of the cross section of the wire under test

can be obtained by making "contour plots." "Contour plots" are made by plotting voltage output, resistance, and reactance of the bridge versus the position on the wire. In obtaining the data for such a plot, the wire is moved through the coil in equal incremental distances. In the case of Fig. 5.1, 1-foot increments were used. If the contour of a shorter section of wire is to be studied in greater detail, smaller increments could be used. At each section the two bridges are balanced and the dials read. When the bridges are balanced, their dials read the resistance and reactance that the bridges "see." Thus, by keeping a running account of the impedance readings of the bridges in moving from section to section and plotting these readings versus section position, a picture of the relative values of the resistance and reactance and how they vary from one section to the next is obtained. Since the resistance and reactance of the wire are dependent on changes in the wire properties such as composition change, surface irregularities, flaws, and dirt, a contour plot therefore gives a qualitative picture of the irregularities of any prescribed length of wire. The data for the voltage contour plot had to be obtained separately from the bridge dial readings. Since the bridge had to be balanced for the next reading at each section, the only voltage output was that caused by the unbalance in moving from one section to another. For the voltage contour plots, the system was balanced on the good end section. Once balanced on the end section, the bridge dials were left untouched as the wire was passed through the test coil from section to section. The voltage output of each bridge at each section was recorded.

Figure 5.1 shows a contour plot of a piece of 0.080-inch-diameter chrome-silicon wire. Except at the 3-foot position where the high-frequency resistance and reactance readings decreased while the corresponding low-frequency readings did not, the curves are all essentially the same. There is no explanation for the discrepancy at the 3-foot section except as always there is the possibility of human error in the recording of the data.

The first eight sections of wire used in the contour plots were sectioned and polished to determine what had caused the high peaks in this region of the contour plots. The results are tabulated below.

Section Position, ft	Description of Results After Sectioning
1	No flaw
2	No flaw .
3	0.002-inch crack
4	0.024-inch crack
5	0.004-inch crack
6	0.004-inch-wide crack
7	No crack
8	No crack

The cracks listed above were very short ones that were caused by improper heat treatment. The discrepancy in the section of 5- and 9-foot positions is most likely due to the fact that in sectioning and polishing a particular section, only one particular cross section of wire is examined as compared to a particular volume of wire approximately 1/4-inch long when the same sample is being tested using the two-frequency flaw detector. Care was taken to make certain that the piece that was sectioned and polished was in the center of the test coil. However, it is possible that a crack was terminating at one of the areas that was being sectioned and polished. In this way a crack could be missed even though it was detected when in the test coil.

The contour plot of voltages shows that the larger cracks are readily indicated and that a representative picture of the wire is obtained. In actual operation of the two-frequency system, the difference voltage is used. The low-frequency bridge "tends to follow" the high-frequency bridge output. However, the contour plots show that the difference voltage is more indicative of the crack depth than either one of the output voltages alone.

The long flat section of the curves for the resistance and reactance indicates a good portion of wire. The irregularities in this region of the wire can be seen in the output voltages but not as changes in the resistance and reactance. The impedance changes were so small that they could not be read on the bridge dials but were of sufficient magnitude to produce output voltages from the bridges.

5.4. TESTING WIRE USING THE TWO-FREQUENCY SYSTEM

The tests in section 5.3 were conducted to obtain contours of how the resistances, reactances, and voltage vary in the high- and low-frequency channels as a function of wire length. The readings obtained were used only to plot the contours of Fig. 5.1 and to obtain initial settings for the bridges.

Recalling that the reason for the two-frequency system was to eliminate the effects of homogeneous composition changes in the wire, the actual length of the wire tested in section 5.3 was relatively short for testing the ability of the two-frequency system to eliminate these effects. It is recalled that the single-frequency system had to be maintained normally at a running balance due to the gradual changes in the wire composition, size, and surface conditions as the wire was passed through the test coil. This gradual change caused the bridge to become unbalanced and thus caused it to lose its detecting ability. The running balance was therefore conceived to circumvent this difficulty. In the two-frequency system, it was expected that the effect of changes in the homogeneous variations in wire composition

would be eliminated by taking the difference voltage of the output of the two bridges.

In preparing the two-frequency system for testing, each bridge was first balanced on a good section of wire. The wire was then passed through the coil a short distance to another good section of wire. In passing from one good section to another, a homogeneous change in the wire caused an output voltage from each bridge. The high- and low-frequency amplifier gains were then adjusted so that the difference voltage would be zero. According to theory, the difference voltage out of the system should be zero for another good piece of wire. This, however, was found not always to be true. It was found that in advancing to a third good section the difference voltage was not zero but was some small value. The value of the difference voltage at times reached a sizable value. This meant that the system could not be adjusted in this manner for continuous testing and that some form of a running balance still had to be used on the two-frequency system. As the wire was being tested, both bridges gradually became unbalanced due to homogeneous change. Since the high-frequency bridge was inherently more sensitive than the low-frequency bridge, it produced a proportionately larger output voltage than the low-frequency bridge which resulted in the difference voltage becoming gradually larger as the level of the two output voltages increased. Since the difference voltage is used as a means of detection, this increase in difference voltage had to be eliminated either by rebalancing the bridges or providing some other means of compensation. In this case, since the difference voltage could not readily be eliminated, compensation was provided by increasing the difference voltage necessary to trigger the point gun as the wire was being tested.

It was found, however, that when testing a single coil of wire at a time, the trigger voltage had to be increased only by a small amount. Thus, the two-frequency system provided partial compensation. However, in moving from one heat to the next, the difference voltage became sufficiently large so that rebalancing of the bridges was essential.

Eighteen coils of .184/.187-inch-diameter chrome-silicon wire were tested on the system. The system was calibrated using a section of .187-inch diameter wire that had a 0.004-inch crack. Using two good sections and the cracked section, it was possible to determine gain settings and the difference voltage produced by a 0.004-inch-deep crack.

Twelve coils of .184/.187-inch-diameter chrome-silicon wire from the American Steel and Wire Company were tested. The results of the test are tabulated in Table 5.1. All the springs that were made from these twelve coils were 100% magnafluxed. No flaws were detected using the magnaflux method of detection. The 59 springs detected from Coil No. H-11488 were magnafluxed and etched; 23 showed surface die scratches.

Six coils of .184/.187-inch-diameter chrome-silicon wire from Washburn Wire Company were also tested. The results of these tests are also tabulated in Table 5.1. All detected springs were returned to the Barnes-Gibson-Raymond Laboratory where they were magnafluxed and etched. When there was some doubt as to whether a scratch or flaw was present, the spring was also sectioned and polished, and then examined under the microscope. Of the 83 springs returned from these 6 coils, 6 springs showed 0.003-inch-deep lap seams, and 12 showed surface scratches. The rest of the springs that were passed by the system were all 100% magnafluxed. None were found to have flaws. Even though there was considerable over-detection, the system had extracted the only 6 faulty springs out of approximately 35,000 produced from the 18 coils. In the case when detection of cracks of 0.008-inch deep and deeper is desired, the sensitivity could have been decreased by decreasing the amplifier gains and a considerable decrease in the amount of over-detection could have been obtained. In the above tests, the sensitivity was set high to detect small seams, and as the above results indicate, under these conditions a very irregular surface condition or dirt in the wire are also sufficient to give an indication.

CONCLUSIONS

The major objective of this project was to establish a satisfactory method of detecting flaws in spring wire that would be independent of the variation in the physical properties that exist in commercially acceptable wire stock. In addition, the final method of test should be competitive in cost with existing methods.

As a results of the work performed on this project, the following conclusions have been drawn:

1. Either the single-frequency system or the two-frequency system is capable of detecting flaws in spring stock.
2. The reason for using the two-frequency system, was to obtain a system that would be insensitive to variations in chemical and physical properties of the wire which may be obtained in the process of producing acceptable spring wire. The results obtained on the two-frequency system to date, while better than the single-frequency system, have not succeeded in separating the seams from acceptable physical variations to the extent that would warrant the additional complexity of equipment needed.
3. The over-detection that results in using either system is due to the wide variations that exist at the present time in commercially accept-

able wire stock. A small crack can be masked by variations in the physical properties of the wire, such as dirt, surface scale, etc. However, inspection of the results on pages 5, 6, and 30 reveal that the over-detection has picked up some of these other imperfections which may in the future be important in the quality control of spring wire.

4. The testing of wire stock can be conducted by untrained personnel with only a brief instruction period. The results obtained using the single-frequency system (see page 6) under these conditions compare favorably with the present magnaflux method of test.

5. Since at the present time, only spot-check testing is performed on commercially acceptable wire stock, it is impossible for a continuous system such as the single-frequency system, to economically compete with a spot-check process. At the present time, the percentage of failures in fabricated items has not warranted the use of a continuous method of testing wire.

SUGGESTIONS FOR FUTURE WORK

If in the future additional developmental work is contemplated, it should be directed toward the construction of a self-balancing single-frequency system. The major difficulty at the present time is the "long-time" drift that occurs due to variations in the physical properties of the wire over extended periods of time. Since seams or cooling cracks are of relatively short length, a long-time-constant servomechanism that would rebalance the bridge on the "long-time" average should lead to a completely automatic wire flaw detector.

APPENDIX

It is the purpose of this appendix to present in detail some of the circuitry used in the construction of the two-frequency flaw detector. The system was constructed so that any one of three high frequencies and any one of three low frequencies could be selected as the two frequencies to be used in performing the measurements. While the usable high- and low-frequency limits were established initially, the optimum values within this range were not known. It was also conjectured that different optimum frequencies may exist for different chemical compositions.

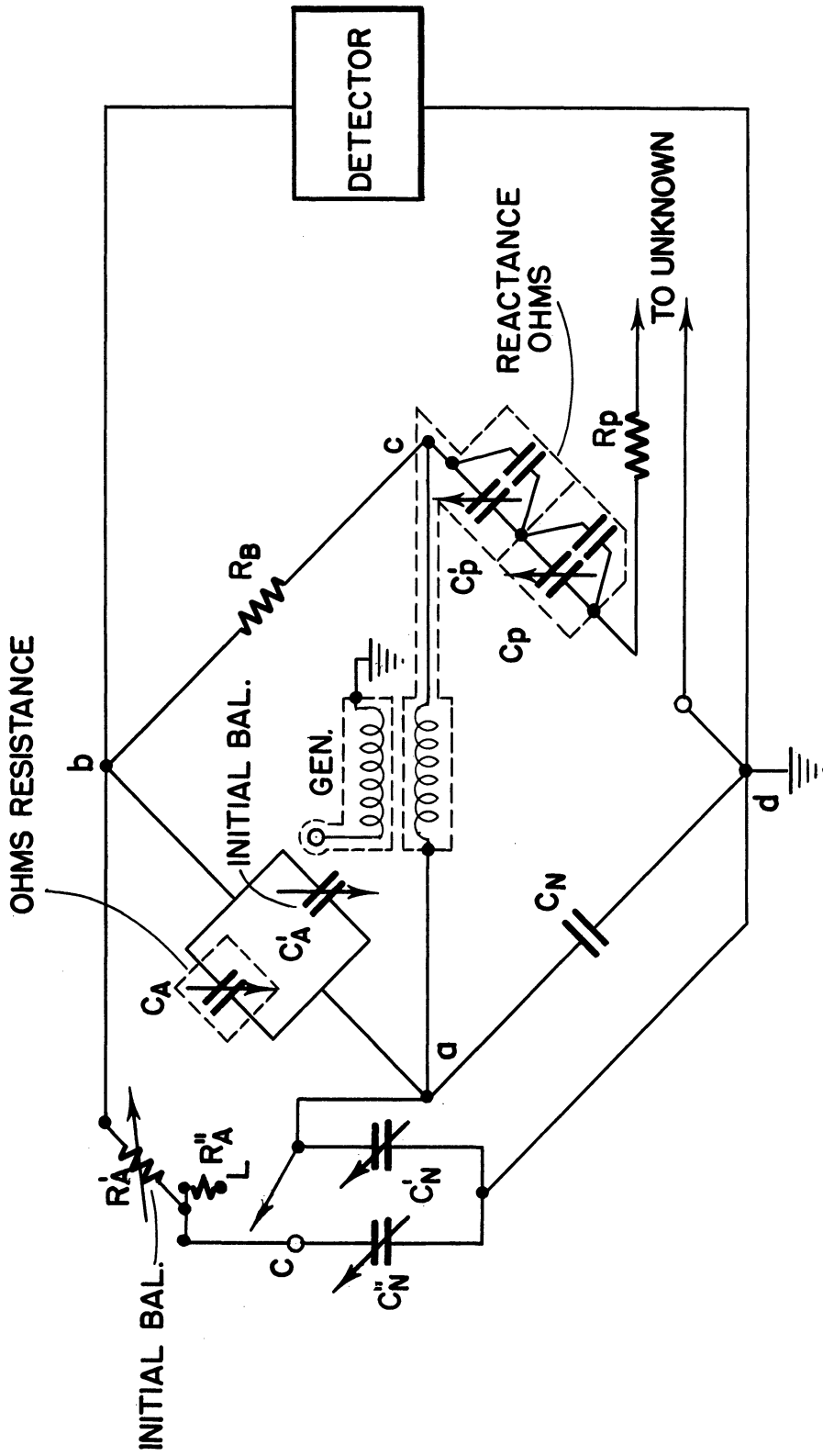
After a limited amount of experimentation, it was found that 1.2 megacycles and 500 kilocycles worked best together on the wire sample tested. Therefore, in the diagrams that follow, the 1.2 megacycles and 0.5 megacycle were used as examples of the typical component used.

A-1. THE GENERAL RADIO 916 AL BRIDGE

Figure A-1 is a schematic of the 916 AL bridge that is used as the impedance detecting device in both the high- and low-frequency channels. The General Radio 916 AL bridge is of the series substitution type for measuring an unknown impedance in the 50-kilocycle—5-megacycle frequency range. This bridge is capable of measuring small impedances accurately. The reason for its use was freedom from drift over extended periods of time. Preliminary tests on other bridges indicated that considerable drift occurred in other makes over extended periods of time. Since the bridge is of a substitution type, it must be initially balanced using a prescribed shorting stub. Once properly balanced, the resistance and reactance of an unknown can be readily determined.

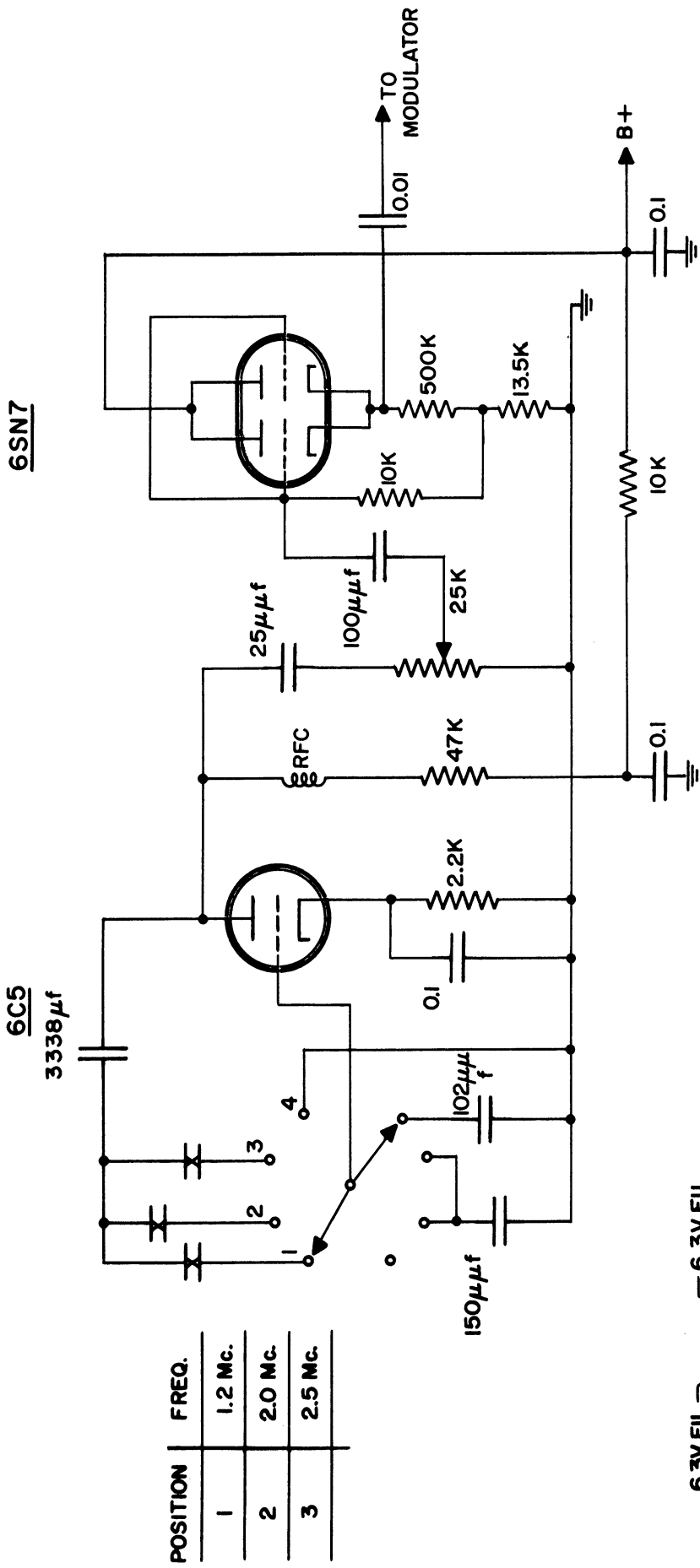
A-2. THE HIGH-FREQUENCY OSCILLATOR

Figure A-2 is a circuit diagram of the high-frequency oscillator. This crystal-controlled oscillator supplies the 1.2-megacycle radio-frequency signal to the high-frequency side. Its output goes to the modulator unit where it is modulated and amplified prior to going to the bridge.

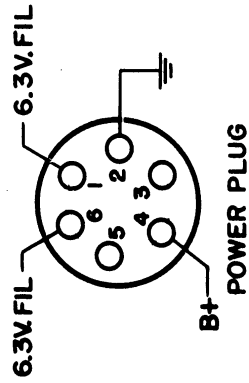


WIRING DIAGRAM OF G.R. 916 AL BRIDGE

Fig. A-1.



POSITION	FREQ.
1	1.2 Mc.
2	2.0 Mc.
3	2.5 Mc.



High Frequency Oscillator

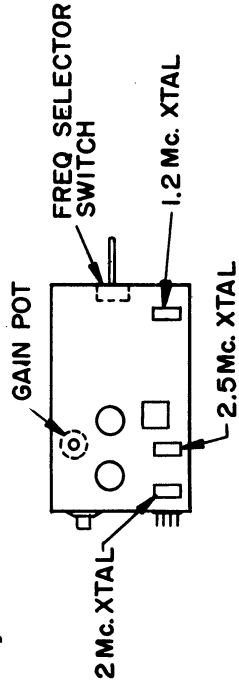


Fig. A-2.

Because the radio-frequency bridges are very critical as to frequency, a crystal-controlled oscillator is necessary. In order to prevent variations in frequency, caused by loading the oscillator, a cathode-follower output stage is used to couple the oscillator to the modulator.

A-3. HIGH-FREQUENCY MODULATOR AND 1000-CPS OSCILLATOR

Figure A-3 is a schematic diagram of the high-frequency modulator and 1000-cps oscillator. The radio-frequency signal from the oscillator is suppressor-grid modulated in the modulator stage. The 1000-cps modulating signal is supplied by the resistance-capacitance phase-shift oscillator. Pot No. 1 allows for the fine adjustment of the oscillator frequency to 1000 cps. Pot Nos. 2 and 3 are the percent modulation adjustment. Modulation is usually maintained at 100%.

The 1.2-megacycle—1000-cps modulated signal output of this unit is fed into the bridge. To match the low input impedance of the bridge, a cathode follower is used as the output stage. Pot No. 4 is the gain control of the unit. The strength of the signal going into the bridge determines the sensitivity of the bridge in terms of an unbalanced output voltage from the bridge. Hence, by adjusting the gain of this unit, the bridge output voltage for a given degree of unbalance can be selected.

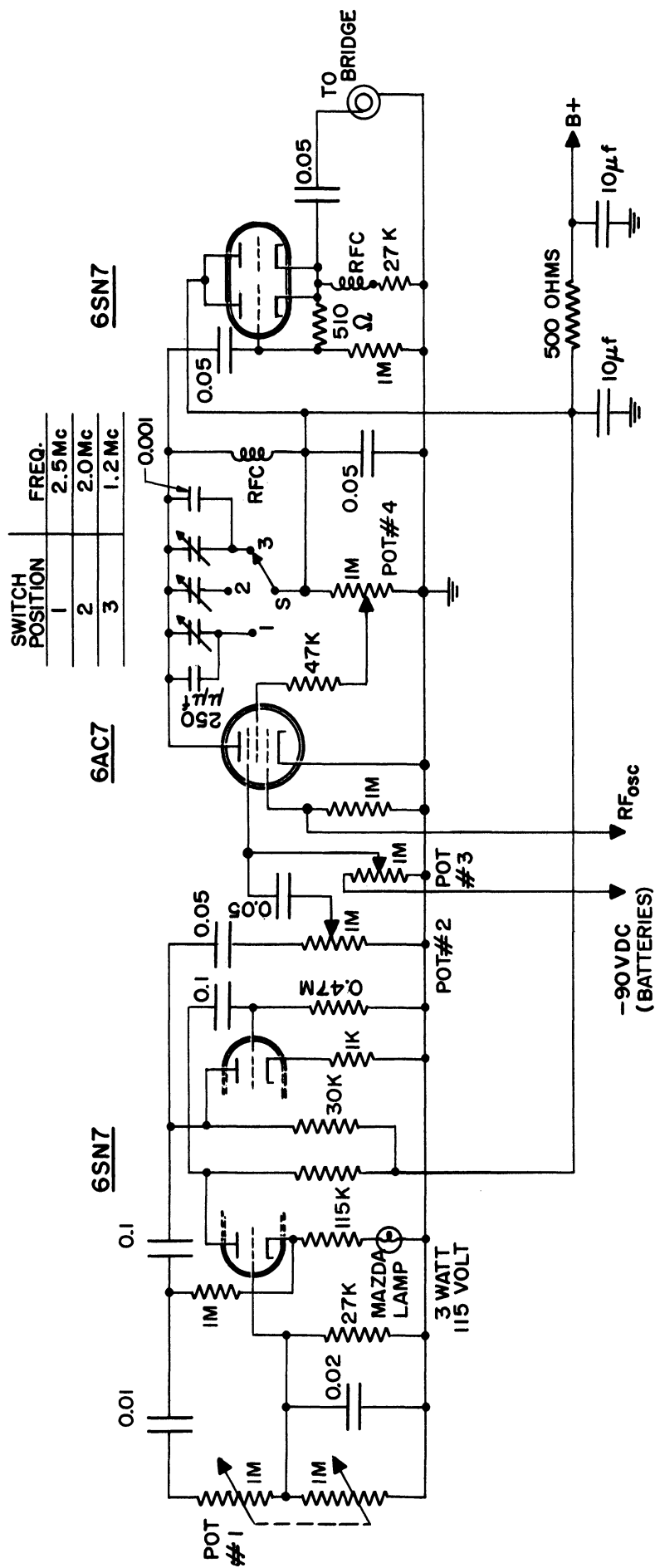
A-4. THE 1.2-MEGACYCLE PRE-AMPLIFIER

Figure A-4 is a schematic diagram of the 1.2-megacycle pre-amplifier. This unit plugs directly into the bridge output jack and is mounted on the bridge. The amount of stray pickup is greatly reduced in this manner. Because of the low level of the output voltage from the bridge, stray pickup is of major concern.

The first stage is a high-gain tuned amplifier stage which amplifies the output of the bridge sufficiently to be sent to the next stage which is the detector stage. After detection, the 1000-cps output signal is sent to the common amplifier. The Q of the tank circuit of this unit has to be high to eliminate harmonics that originate in the bridge. The Q of a coil is defined as the ratio of reactance to resistance of a given coil.

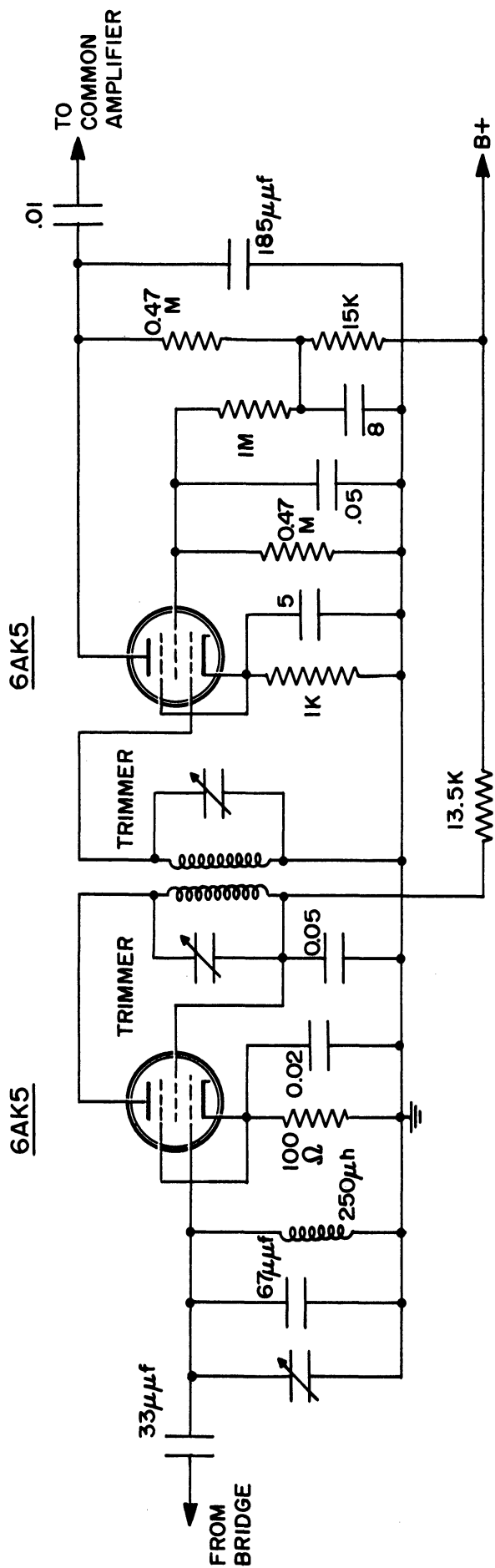
A-5. THE LOW-FREQUENCY OSCILLATOR

Figure A-5 is a schematic diagram of the low-frequency oscillator. This crystal-controlled oscillator supplies 100- 250- or 500-kilocycle radio-frequency signal to the low-frequency side. Its output goes to the modulator



High Frequency 1000~ Oscillator and Modulator

Fig. A-3.



Pre-Amplifier 1.2 Mc.
Fig. A-4.

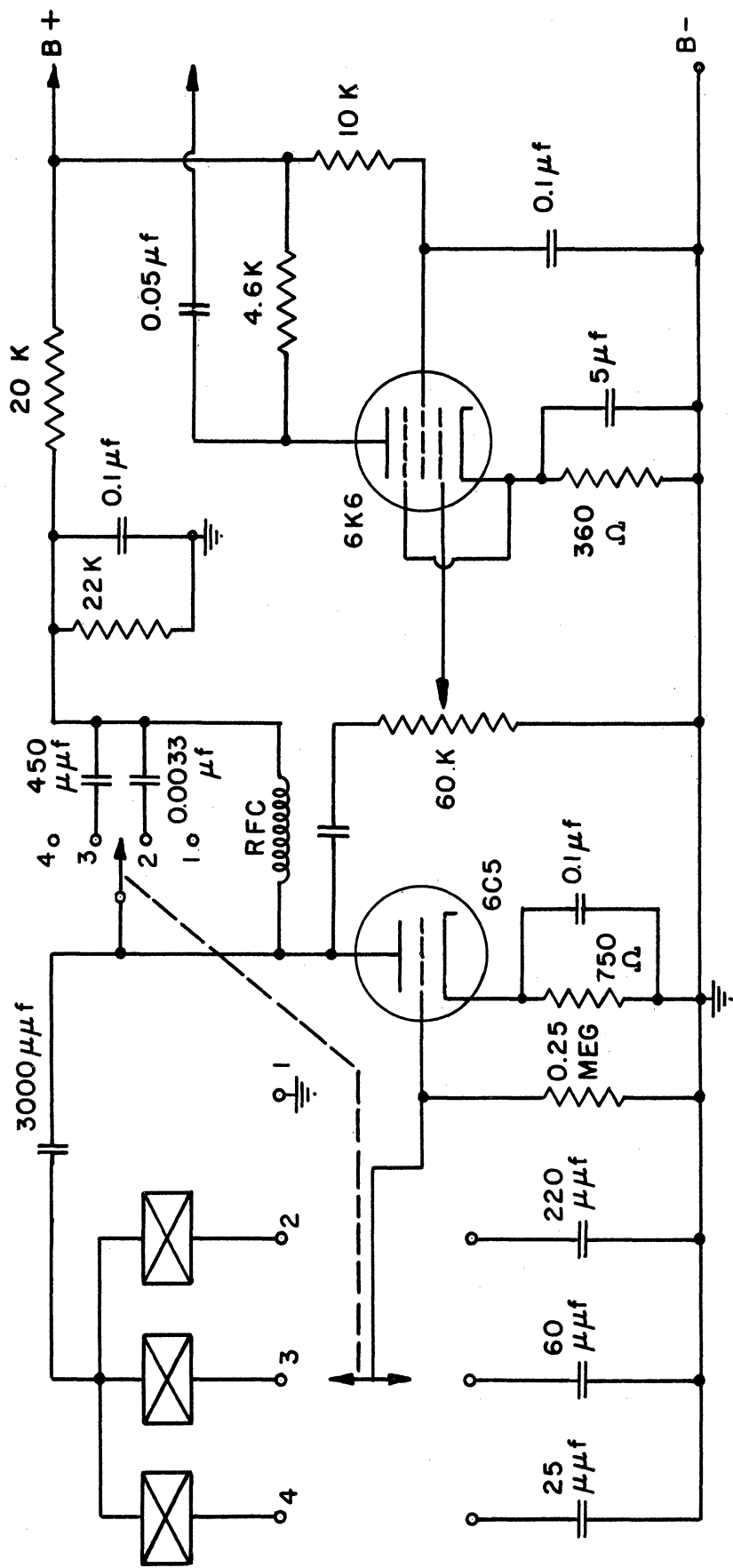


Fig. A-5. Low-Frequency Oscillator Circuit Diagram.

unit where it is modulated and amplified prior to going to the bridge. A cathode follower is used as the output stage to prevent loading of the oscillator. As in the case of the high-frequency oscillator, the main concern is frequency stability.

A-6. THE LOW-FREQUENCY MODULATOR AND 400-CPS OSCILLATOR

Figure A-6 is a schematic diagram of the low-frequency modulator and 400-cps oscillator. The 500-kilocycle radio-frequency signal from the oscillator is suppressor-grid modulated and amplified in this unit. The 400-cps modulating signal is supplied by a resistance-capacitance phase-shift oscillator; the 500-kilocycle-400-cps modulated signal is sent to the bridge. The gain control of the unit affords the necessary control over the signal strength into the bridge so that the bridge's sensitivity can be controlled in a manner similar to the high-frequency side. It was found necessary to set the gain control at its maximum value in order to give the bridge enough sensitivity at 500 kilocycles.

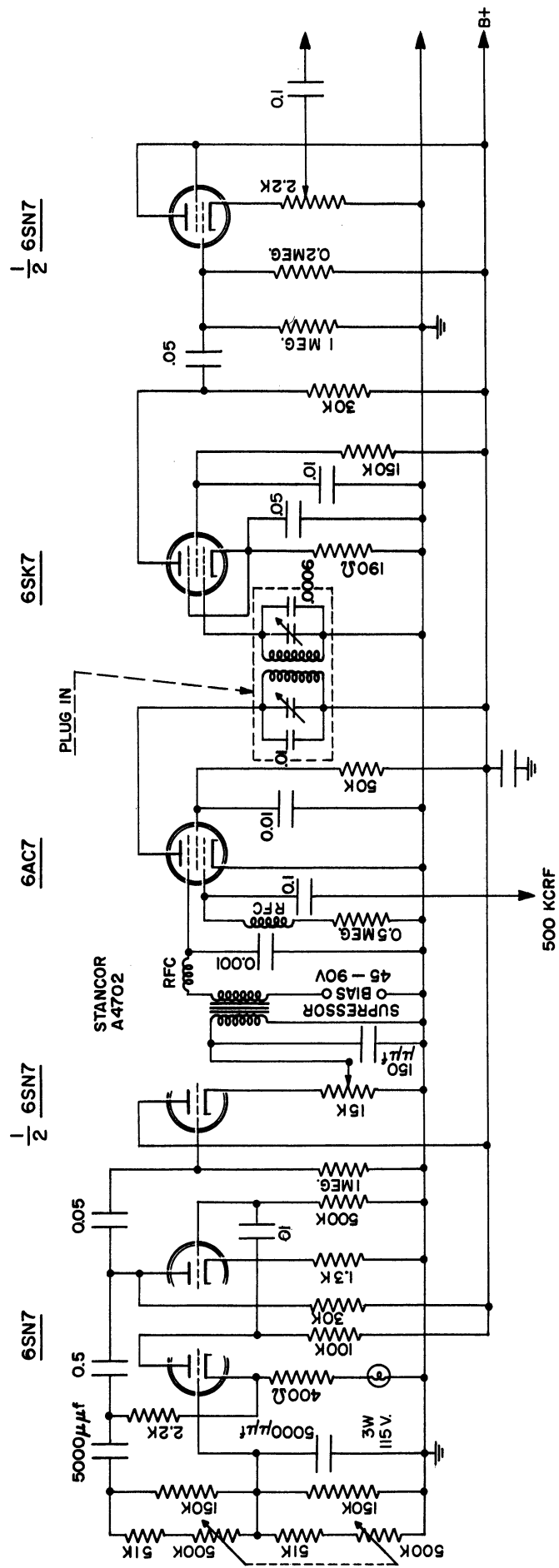
A-7. 500-KILOCYCLE PRE-AMPLIFIERS

Figure A-7 is the schematic diagram of the 500-kilocycle pre-amplifier. This unit plugs directly into the bridge output jack and is mounted on the bridge. This close proximity to the bridge reduces the possible stray pickup.

The first stage is a high-gain tuned amplifier stage which amplifies the output from the bridge sufficiently so that it can be fed directly to a detector stage. After detection, the 400-cps output signal is sent to the common amplifier.

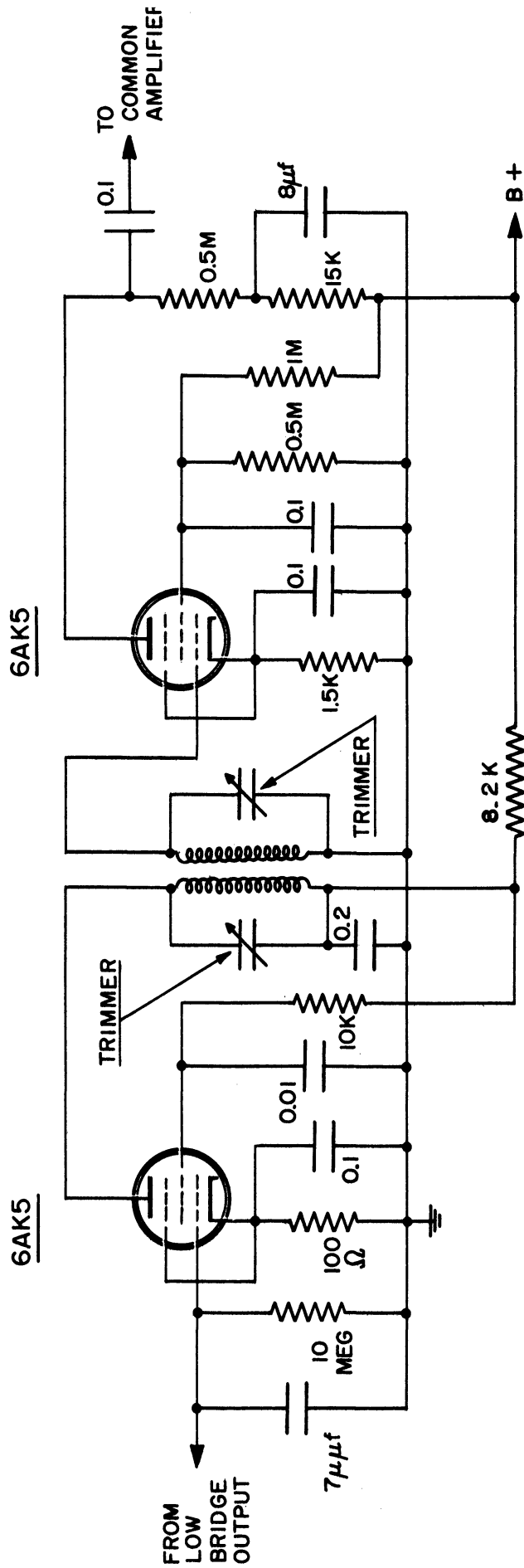
A-8. THE COMMON AMPLIFIER

Figure A-8 is a schematic diagram of the common amplifier for both systems. This unit amplifies simultaneously the 400- and 1000-cps outputs of the pre-amplifiers. It contains two stages of amplification. The gain of the unit is controlled by a double potentiometer in the grid circuit of the second stage. The output stage is a cathode follower. The gain through this unit raises the levels of the signals high enough so that rectification of these signals in the audio filter and difference amplifier unit will yield a usable level of d-c voltage.



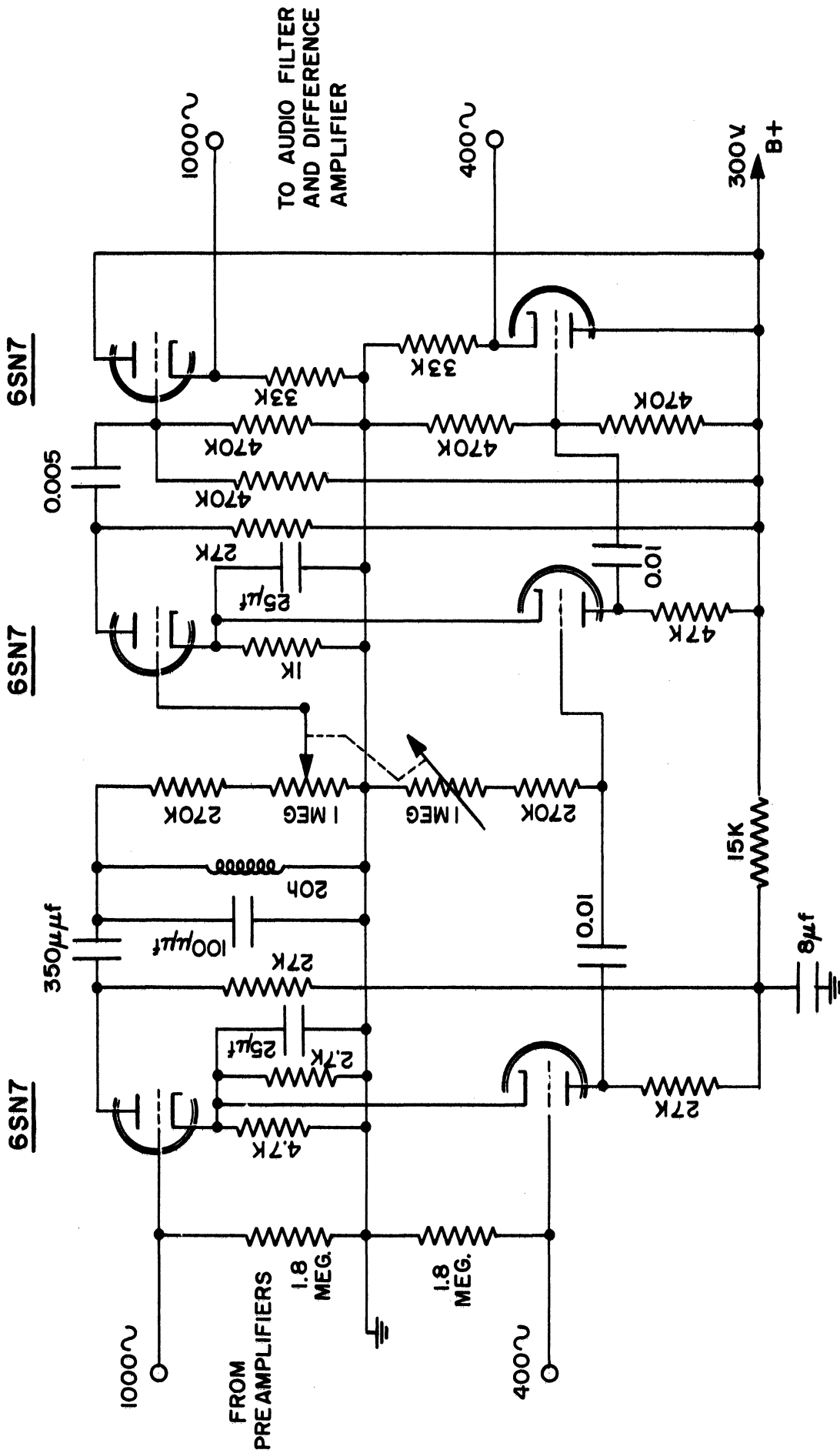
Low Frequency 400~ Oscillator and Modulator

Fig. A-6.



Pre-Amplifier 500 Kc

Fig. A-7.



Common Amplifier

Fig. A-8.

A-9. THE AUDIO FILTER AND DIFFERENCE AMPLIFIER

Figure A-9 is the schematic diagram of the audio filter difference amplifier. The input to this unit contains two band-pass filters; one for 400 cps and the other for 1000 cps. They are used for positive separation of the two signals. Positive separation is necessary because each signal is a representative of the output voltage of its bridge source. In the rectification of each signal to the direct current, a corresponding d-c voltage is desired from each. Any intermingling of the two signals prior to rectification would not yield d-c voltages that were true representatives of the two signals.

The final stage, which is the differential amplifier can be adjusted to zero even though the two d-c voltages may not be equal. The adjustment is necessary since even though the bridge outputs may be identical, the probability of having both d-c voltages exactly equal is very small because of the many stages of amplification between the bridge and the rectifier. The output of this unit goes to the control chassis and meter circuit.

A-10. THE CONTROL CHASSIS

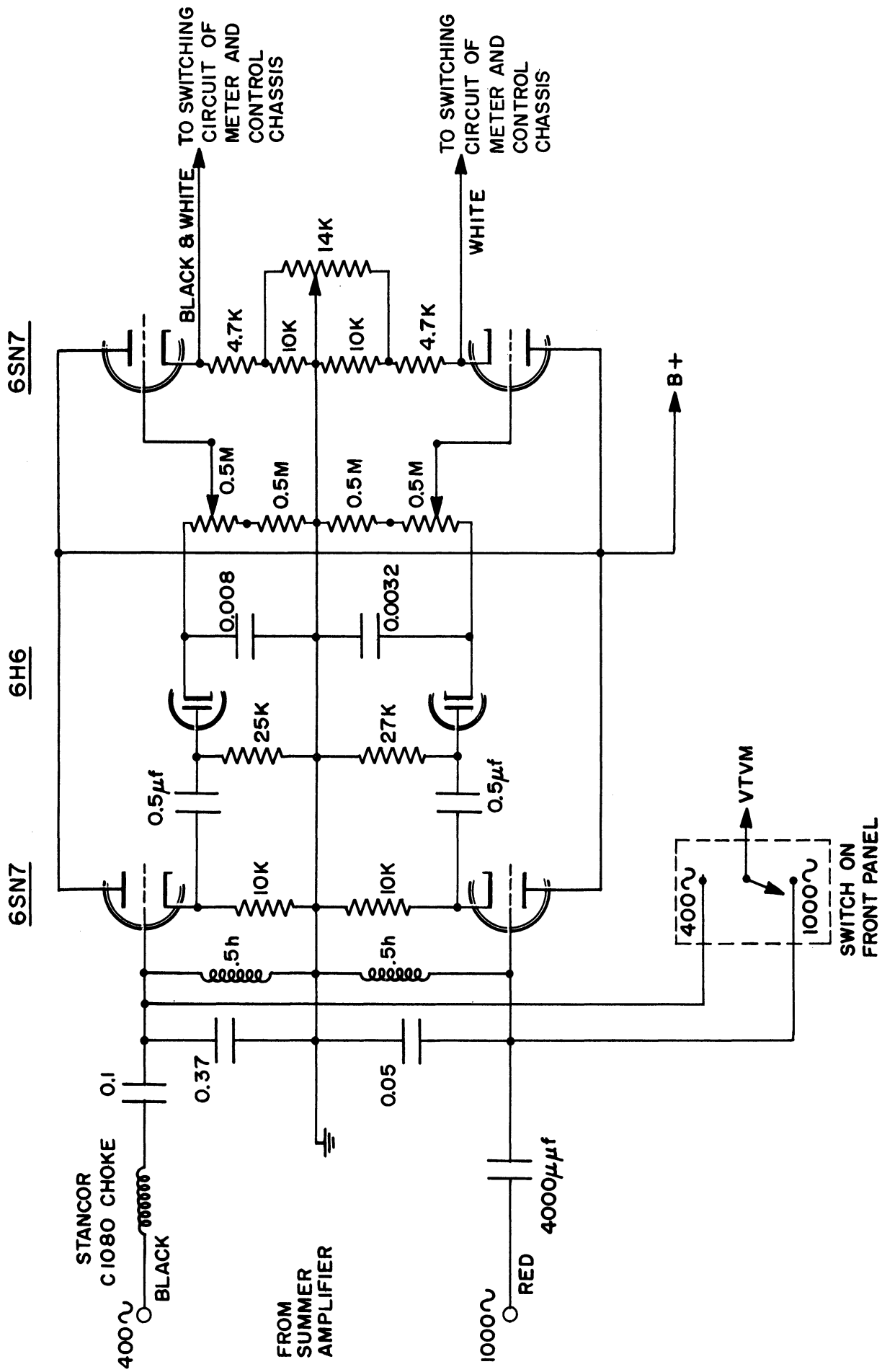
Figure A-10 is a wiring diagram of the control chassis of this unit which contains the thyatron circuit that is used to activate the marking solenoid. The thyatron circuit can be adjusted to fire at a wide range of difference voltages. Knowing the minimum-sized crack to be detected, the difference voltage can be adjusted so that the tester will trigger when a crack of the minimum size or deeper is encountered.

A-11. THE METER CIRCUIT

Figure A-11 is a schematic diagram of the meter circuit; the meter circuit is used primarily for monitoring and checking out the system. The meter can be selected to read the d-c voltage corresponding to either the 400- or 1000-cps signal or the difference voltage. Because the difference voltage is above ground by the amount of the smallest of the two signals, it requires the meter circuit to have an isolated ground from the rest of the system. To accomplish this separate ground, the meter circuit has its own power supply isolated from the rest of the system. The power supply is needed for the protective circuit for the meter from accidental over-voltages.

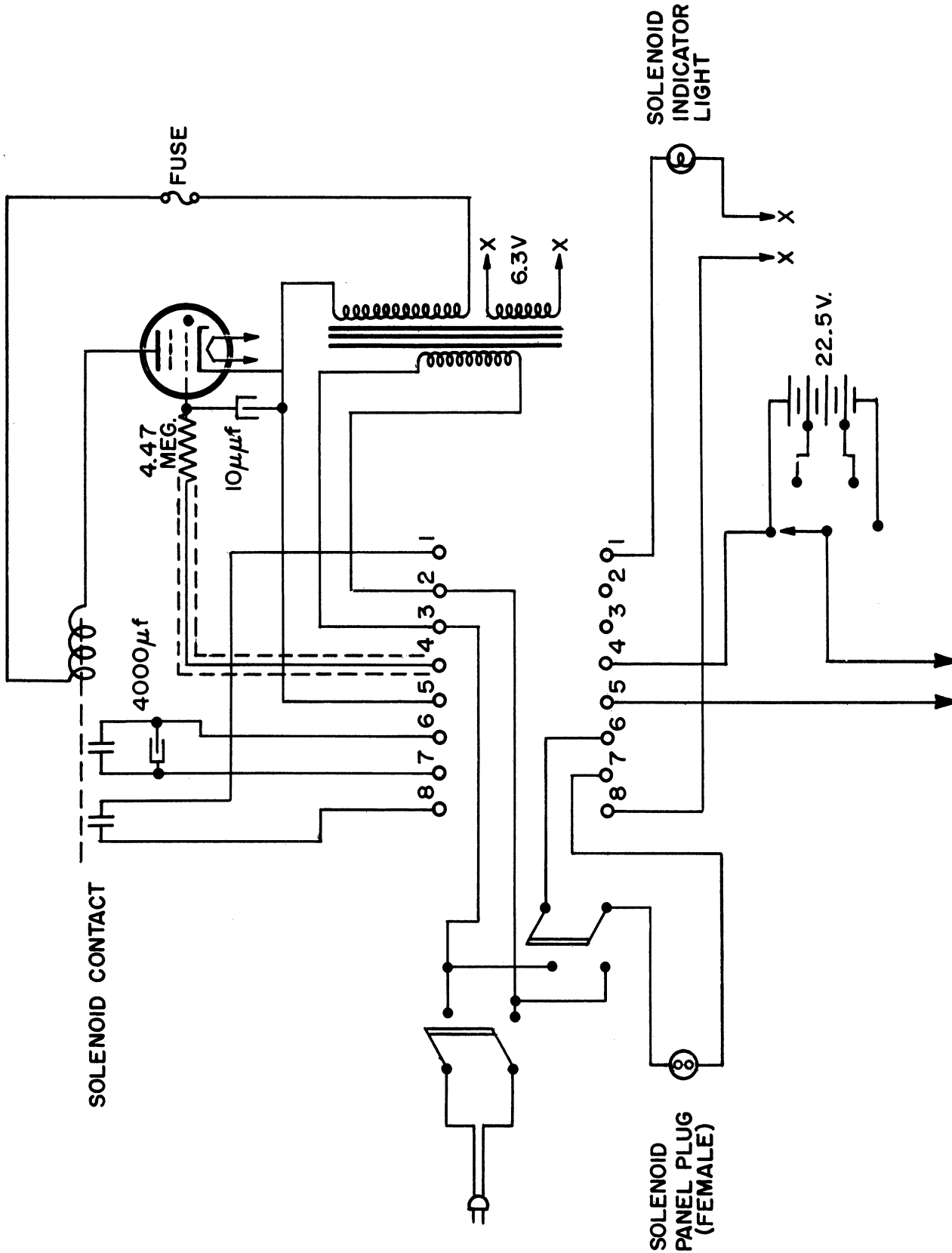
A-12. POWER SUPPLIES

Figure A-12 is the circuit diagram for two Model 28 Lambda power



Audio Filter and Difference Amplifier

Fig. A-9.

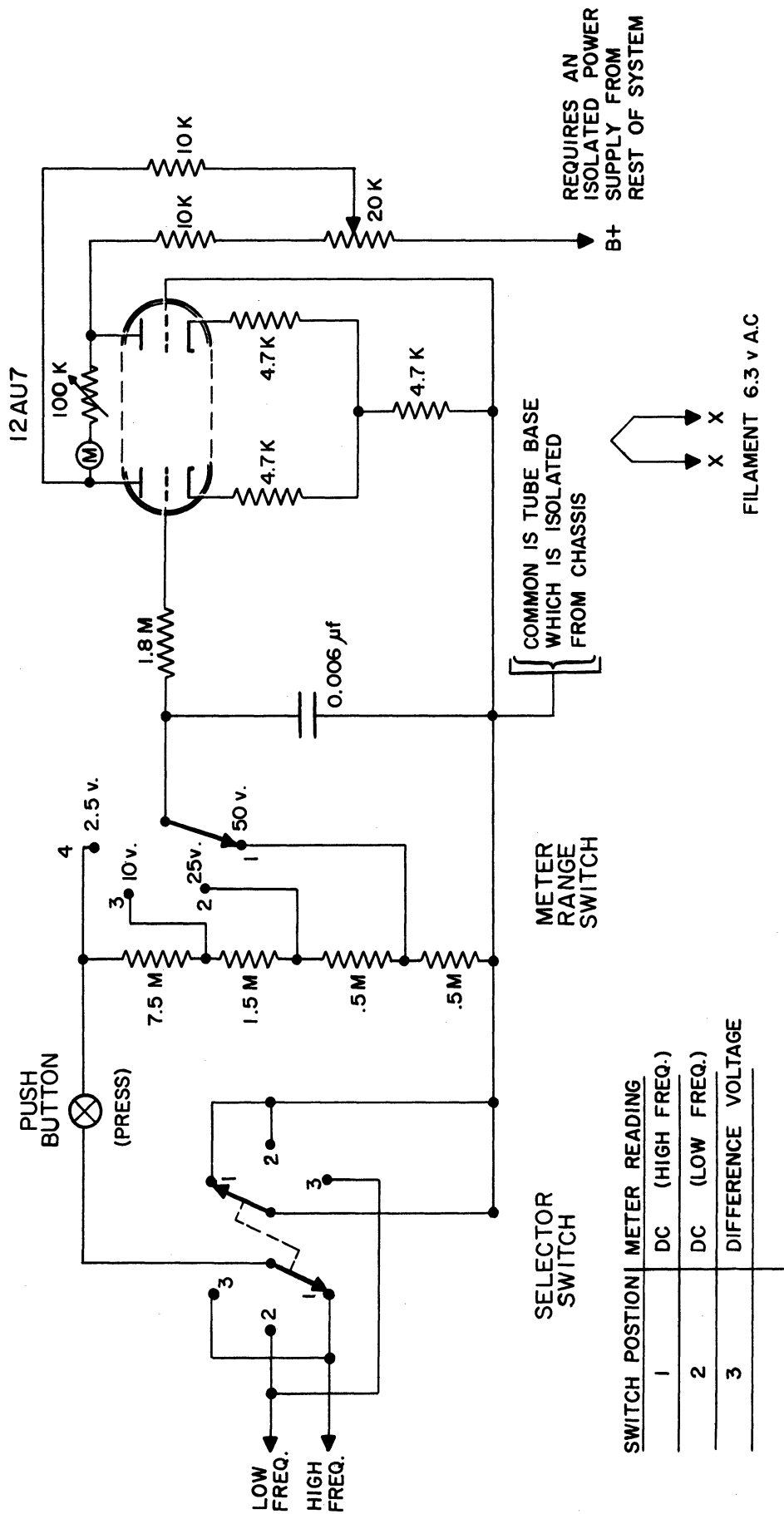


TO DIFFERENCE
AMPLIFIER

Control Chassis

Fig. A-10.

METER 0-50 μ AMP.



Meter Circuit

Fig. A-11.

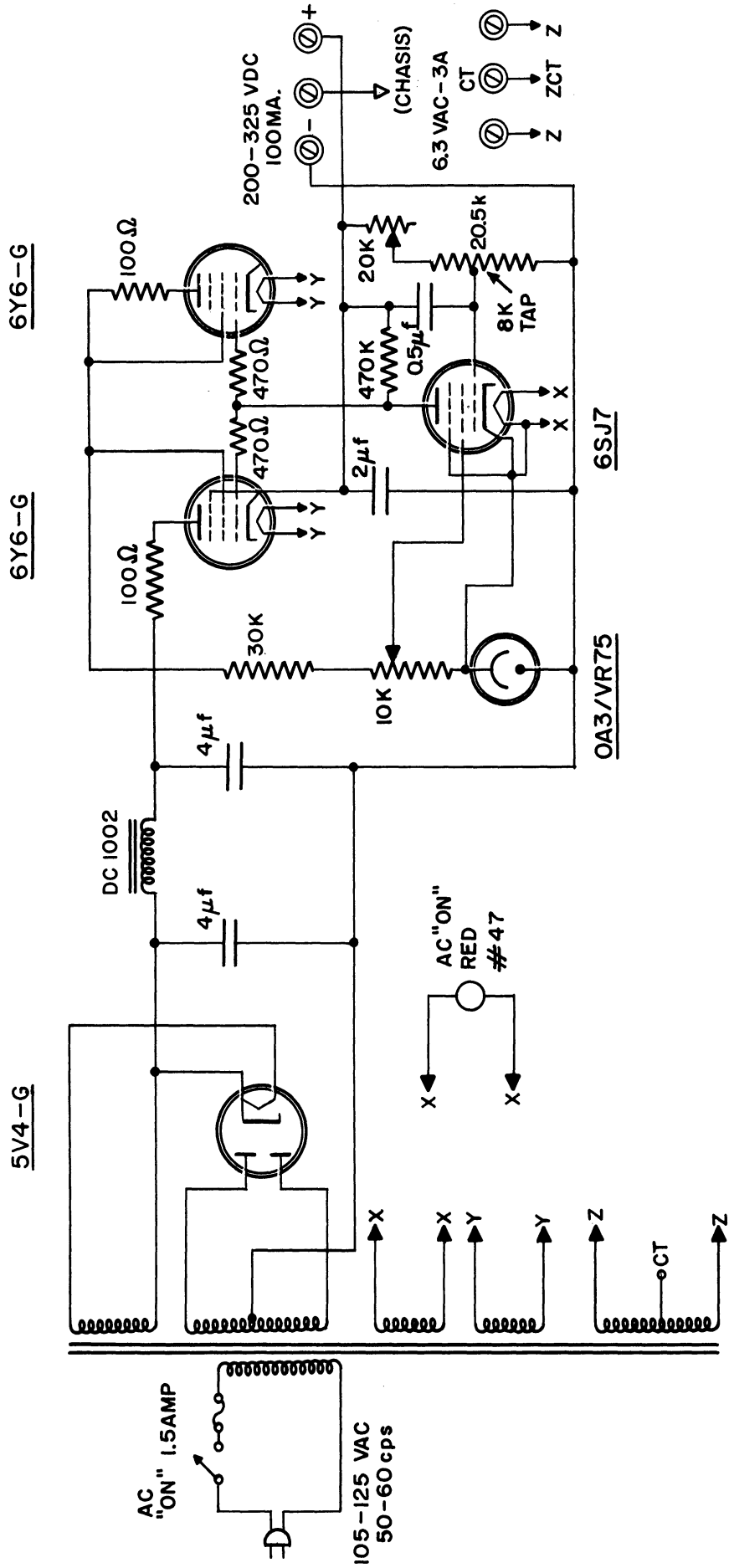


Fig. A-12. Power Supply Lambda Model 28.

supplies that were used without modification. It was found that the use of the same supply for both the high- and low-frequency sides of the system caused some interaction between the two channels which greatly added to the amount of noise in the system. Hence, each side had its own power supply. The meter circuit required a third supply whose ground had to be isolated from the rest of the system.

BIBLIOGRAPHY

1. Watkins, Kermit, and Paivinen, John, "Progress Report on Wire Flaw Detection", (see Appendix), Univ. of Mich., Ann Arbor, Eng. Res. Inst. Project M685-A, July, 1950.
2. Kazda, L. F., "Wire Flaw Detection", Final Report, Univ. of Mich., Ann Arbor, Eng. Res. Inst. Project M685-A, September, 1951.
3. Knern, N.C., "Electrical Detection of Flaws in Metal", Metals and Alloys, 12, No. 4 (October, 1940).
4. Jupe, J. H., "Crack Detector for Production Testing", Electronics, 18 (October, 1945).
5. O'Dell, D. T., "Apparatus for the Detection of Splits in Tungsten Wire", Journal of Scientific Instruments, 20 (September, 1943).

